

LEVEL III



AD-E430264

AD A 072163

TECHNICAL REPORT ARBRL-TR-02165

(Supersedes IMR No. 583)

**IMPROVING THE FLIGHT PERFORMANCE
OF PROJECTILES**

Anders S. Platou

May 1979



**US ARMY ARMAMENT RESEARCH AND DEVELOPMENT COMMAND
BALLISTIC RESEARCH LABORATORY
ABERDEEN PROVING GROUND, MARYLAND**

Approved for public release; distribution unlimited.

**D D C
RECEIVED
AUG 2 1979
D**

DDC FILE COPY

79 07 16 011

Destroy this report when it is no longer needed.
Do not return it to the originator.

Secondary distribution of this report by originating
or sponsoring activity is prohibited.

Additional copies of this report may be obtained
from the National Technical Information Service,
U.S. Department of Commerce, Springfield, Virginia
22151.

The findings in this report are not to be construed as
an official Department of the Army position, unless
so designated by other authorized documents.

*The use of trade names or manufacturers' names in this report
does not constitute endorsement of any commercial product.*

UNCLASSIFIED

SECURITY CLASSIFICATION OF THIS PAGE (When Data Entered)

REPORT DOCUMENTATION PAGE		READ INSTRUCTIONS BEFORE COMPLETING FORM
1. REPORT NUMBER TECHNICAL REPORT ARBRL-TR-02165 ✓	2. GOVT ACCESSION NO.	3. RECIPIENT'S CATALOG NUMBER
4. TITLE (and Subtitle) IMPROVING THE FLIGHT PERFORMANCE OF PROJECTILES		5. TYPE OF REPORT & PERIOD COVERED Final
7. AUTHOR(s) Anders S. Platou		6. PERFORMING ORG. REPORT NUMBER
9. PERFORMING ORGANIZATION NAME AND ADDRESS ✓ U.S. Army Ballistic Research Laboratory (ATTN: DRDAR-BLL) Aberdeen Proving Ground, Maryland 21005		8. CONTRACT OR GRANT NUMBER(s)
11. CONTROLLING OFFICE NAME AND ADDRESS U.S. Army Armament Research & Development Command U.S. Army Ballistic Research Laboratory (ATTN: DRDAR-BL) Aberdeen Proving Ground, MD 21005		10. PROGRAM ELEMENT, PROJECT, TASK AREA & WORK UNIT NUMBERS RDT&E 1L161102AH80
14. MONITORING AGENCY NAME & ADDRESS (if different from Controlling Office)		12. REPORT DATE MAY 1979
		13. NUMBER OF PAGES 71
		15. SECURITY CLASS. (of this report) Unclassified
		15a. DECLASSIFICATION/DOWNGRADING SCHEDULE
16. DISTRIBUTION STATEMENT (of this Report) Approved for public release, distribution unlimited.		
17. DISTRIBUTION STATEMENT (of the abstract entered in Block 20, if different from Report)		
18. SUPPLEMENTARY NOTES This BRL Technical Report supersedes BRL Interim Memorandum Report No. 583 dated December 1977.		
19. KEY WORDS (Continue on reverse side if necessary; and identify by block number) Army Ordnance Projectile Aeroballistics		
20. ABSTRACT (Continue on reverse side if necessary and identify by block number) (1cb) The BRL has been conducting experiments on spin stabilized projectiles using a new boattail shape called the Non-Conical Boattail. This boattail improves the aeroballistic characteristics of the projectile so that longer ranges are attained and heavier payloads can be flown to the target with good accuracy. Many of these experiments have been carried out on 155mm diameter full bore projectiles, but the aerodynamic characteristics can be applied to this configuration in any diameter including subcalibered projectiles. (Continued)		

DD FORM 1473 1 JAN 73 EDITION OF 1 NOV 65 IS OBSOLETE

UNCLASSIFIED

SECURITY CLASSIFICATION OF THIS PAGE (When Data Entered)

UNCLASSIFIED

SECURITY CLASSIFICATION OF THIS PAGE(When Data Entered)

20. ABSTRACT (Continued):

The new boattail also provides a better configuration than a conical boattail for imparting spin as well as forward velocity to the projectile through a saboting system. In this report, the aerodynamic and aeroballistic characteristics of the new projectile as obtained from aeroballistic ranges, wind tunnels, and full range flights are summarized and compared to a similar conical boattail projectile.

UNCLASSIFIED

SECURITY CLASSIFICATION OF THIS PAGE(When Data Entered)

LIST OF ILLUSTRATIONS

<u>Figure</u>	<u>Page</u>
1. The 155mm M549 Projectile	30
2. The 155mm SRC Projectile	31
3. The 155mm Non-Conical Boattail Projectile-A (NCB-A)	32
4. The 155mm Non-Conical Boattail Projectile-B (NCB-B)	33
5. The 105mm and 155mm Models of the Non-Conical Boattail Projectile-A (NCB-A)	34
6. Free Flight and Ground Test Facilities Reynolds Numbers	35
7. The Cross-Section Area Distribution of a Conical and Non-Conical Boattail	36
8. The Zero Yaw Drag Coefficient of the NCB-A and M549 Projectiles	37
9. The Low Yaw Pitching Moment Coefficients of the NCB-A and M549 Projectiles	38
10. The Polar Characteristics of the NCB-A at $M = .851$, $R_d = 2.59 \times 10^6$	39
11. The Polar Characteristics of the NCB-A at $M = .90$, $R_d = 2.50 \times 10^6$	40
12. The Polar Characteristics of the NCB-A at $M = .951$, $R_d = 2.47 \times 10^6$	41
13. The Polar Characteristics of the NCB-A at $M = .978$, $R_d = 2.03 \times 10^6$	42
14. The Polar Characteristics of the NCB-A at $M = 1.76$, $R_d = .97 \times 10^6$	43
15. The Polar Characteristics of the NCB-A at $M = 2.27$, $R_d = 1.06 \times 10^6$	44
16. The Variation in Normal Force Coefficient With Spin on the NCB-A With a 1/20 Caliber Twist Boattail at $M = .95$	45
17. The Variation in Pitching Moment Coefficient With Spin on the NCB-A With a 1/20 Caliber Twist Boattail at $M = .95$	46

LIST OF ILLUSTRATIONS (Continued)

<u>Figure</u>	<u>Page</u>
18. The Variation of the Normal Force Coefficient With Spin on the NCB-A With a Straight Boattail at $M = .95$	47
19. The Variation of the Pitching Moment Coefficient With Spin on the NCB-A With a Straight Boattail	48
20. The Pitch Damping Moment Coefficient of the NCB-A Compared to the M549 at Small Angles of Attack, $pd/V = .314$	49
21. The Side and Magnus Forces on a Non-Conical Boattail Projectile, $\alpha > 0$	50
22. The Magnus and Side Forces Acting on a Triangular Boattailed Projectile at Various Spins (pd/V)	51
23. The Yawing Force and Moment Zero Spin Offset at $M = 1.76$ and 2.27 , $R_d = 1 \times 10^6$ of the NCB-A	52
24. The Magnus Spin Slopes of the NCB-A at $M = 1.76$, $R_d = .97 \times 10^6$, $pd/V = .314$	53
25. The Effect of Zero Spin Offset on the Yawing Force and Moment at $M = 1.76$ of the NCB-A	54
26. The Yawing Moment Coefficient of the NCB-A Compared to the M549 at Low Angles of Attack	55
27. The Effect of the Side and Pitch Damping Moments on the Damping Rates (λ_F and λ_S) of the Epicyclic Arms, $M = .95$	56
28. The Effect of the Side and Pitch Damping Moments on the Damping Rates (λ_F and λ_S) of the Epicyclic Arms, $M = 1.76$	57
29a. Trajectory and Velocity of the NCB-A, $M = .98$, Q.E. = 45° , $\rho = .997 \text{ kg/m}^3$ (Tonopah)	58
29b. The NCB-A Projectile Yawing Motion, Flight 11, $M = .98$, Q.E. = 45° , $\rho = .997 \text{ kg/m}^3$ (Tonopah)	59
29c. The NCB-A Projectile Spin, Flight 11, $M = .98$, Q.E. = 45° , $\rho = .997 \text{ kg/m}^3$ (Tonopah)	60

LIST OF ILLUSTRATIONS (Concluded)

<u>Figure</u>	<u>Page</u>
30a. Trajectory and Velocity of the NCB-A, M = 1.8, Q.E. = 45°, $\rho = .997 \text{ kg/m}^3$ (Tonopah)	61
30b. The NCB-A Yawing Motion, Flight 20, M = 1.8, Q.E. = 45°, $\rho = .997 \text{ kg/m}^3$ (Tonopah)	62
30c. The NCB-A Projectile Spin, Flight 20, M = 1.8, Q.E. = 45°, $\rho = .997 \text{ kg/m}^3$ (Tonopah)	63

LIST OF TABLES

<u>Table</u>	<u>Page</u>
1. Physical Characteristics of the Various Projectiles	22
2. Aerodynamic Parameters of the 105mm NCB-A Projectile With a 1/20 Caliber Twisted Triangular Boattail	23
3. Aerodynamic Parameters of the 155mm NCB-A Projectile With a 1/20 Caliber Twisted Triangular Boattail	24
4. Aeroballistic Parameters of the 105mm NCB-A Projectile With a 1/20 Caliber Twisted Triangular Boattail and $pd/V = .314$	25
5. Aeroballistic Parameters of the 155mm NCB-A Projectile With a 1/20 Caliber Twisted Triangular Boattail and $pd/V = .314$	26
6. Rolling Moment Coefficients of the NCB-A	27
7. Aerodynamic Data Obtained from Yawsonde Records	27
8. The Impact Data from the NCB-A	28

I. INTRODUCTION

During the past few years the Ballistic Research Laboratory (BRL) has conducted a series of tests to investigate the use of a more aerodynamically efficient, non-conical boattail on spin stabilized projectiles. The new boattail decreases the drag, pitching moment, and Magnus moments acting on the full projectile^{1,2} and improves the projectile flight characteristics by a significant amount. This boattail uses twisted "flat" surfaces to taper the cylindrical projectile body to a triangular base. The "flat" surfaces produce additional aerodynamic lift on the rear of the projectile which in turn decreases the pitching moment. The lower pitching moment increases the gyroscopic stability of a projectile having the same physical characteristics as a conical boattailed projectile, or the lower pitching moment can be traded for increased projectile length. This boattail also creates lower Magnus or yawing moments which in turn produces improved dynamic stability. During the wind tunnel, aeroballistic range, and full range tests, many of the aerodynamic characteristics of a 155mm projectile using the new boattail have been determined. This report presents these characteristics and shows how these characteristics improve the flight performance of the projectile.

Other advantages of the non-conical boattail which are obvious, but have not yet been fully investigated are:

1. Increased wheel bearing is available due to portions of the boattail being at or close to full bore diameter. This will decrease inbore balloting and reduce the first maximum yaw of the projectile.
2. These boattails also provide a good mechanism for imparting full spin as well as forward velocity to a projectile through a discarding sabot design.

II. THE PROJECTILE CONFIGURATION

To explore the use of the non-conical boattail on large caliber projectiles, the BRL chose the following design criteria.

1. Anders S. Platou, "An Improved Projectile Boattail," BRL Memorandum Report No. 2395, July 1974, U.S. Army Ballistic Research Laboratory, Aberdeen Proving Ground, Maryland. AD 785520. Also, ADPA 1st International Symposium on Ballistics, 13-15 November 1974, Orlando, Florida.
2. Anders S. Platou and George I. T. Nielsen, "An Improved Projectile Boattail. Part II," BRL Report No. 1866, March 1976, U.S. Army Ballistic Research Laboratory, Aberdeen Proving Ground, Maryland. AD A024073.

Using known large caliber, low drag projectiles with a conical boattail as references, design two similar shaped projectiles using the new boattail. The projectiles should be longer than the reference projectiles, for added payload potential, but must have adequate gyroscopic stability for good flight characteristics. The projectile will have the same weight and center of gravity location from the projectile nose as the reference projectiles.

The BRL selected as reference projectiles, the 155mm 5.7 caliber long M549³ (Figure 1) and the 155mm 6.1 caliber long SRC projectile (Figure 2) now being manufactured by the Space Research Corporation. The new projectile configurations with the non-conical boattails lengthen the reference projectiles by one-half caliber. The copper rotating band of the M549 configuration is moved forward by .85 caliber to accommodate the 2.036 caliber long non-conical boattail (Figure 3). On the SRC configuration the copper rotating band is replaced with a plastic discarding rotating band. So far, 46 of the 155mm M549 projectiles with the new boattail, henceforth called the non-conical projectile "A" (NCB-A) have been flown over full ranges. Flights of the SRC projectile with a non-conical boattail (Figure 4), henceforth called non-conical boattail projectile "B" (NCB-B) are in progress. This paper presents only the information obtained on the NCB-A and compares it with the M549.

Initially, 20mm solid aluminum models of the non-conical boattail configurations were built for aerodynamic data flights in the BRL Aerodynamics Range. The small model diameter decreased the Reynolds number proportionately, but permitted an early look and comparison with the conical boattail configuration⁴. These results proved the aerodynamic advantage of the new boattail and encouraged us to continue the program. 105mm and 155mm models of the NCB-A configuration have been designed and built for range and free flight firings (Figure 5). Spinning wind tunnel models have been designed and built to obtain pitch and Magnus data at transonic and supersonic speeds.

The 105mm and 155mm projectile physical characteristics are given in Table 1. The projectiles were designed to have the same center of gravity location from the nose (3.5 calibers) and for each size to have approximately the same weight. Since the 105mm projectiles were to be

3. R. Kline, W. R. Herrmann, and V. Oskay, "A Determination of the Aerodynamic Coefficients of the 155mm, M549 Projectile," Technical Report No. 4764, November 1974, Picatinny Arsenal, Dover, New Jersey. AD B002073L.
4. Anders S. Platou, "An Improved Projectile Boattail. Part III," BRL Memorandum Report No. 2644, July 1976, U.S. Army Ballistic Research Laboratory, Aberdeen Proving Ground, Maryland. AD B012781L.

flown only in the BRL Transonic Range for aerodynamic data, their moments of inertia were tailored to give each projectile a minimum gyroscopic stability of approximately 1.5*. Since the 155mm projectiles were to be flown to full ranges to obtain their flight characteristics under various flight conditions, their moments of inertia were tailored to give each projectile a minimum gyroscopic stability between 1.1 to 1.2 at Nicolet ($\rho = 1.320 \text{ kg/m}^3$) and 1.35 at Tonopah ($\rho = .997 \text{ kg/m}^3$). Projectiles flown in the BRL Transonic Range had the same physical characteristics as those flown at Tonopah so their minimum gyroscopic stability was 1.1. Seventeen of the 105mm NCB-A projectiles and eleven of the 155mm NCB-A projectiles were flown in the BRL Transonic Range for aerodynamic data⁵ (Tables 2, 3, 4, and 5), charge assessment, and metal parts integrity. Six of the NCB-A projectiles were launched at Nicolet, Canada⁶ on 10 February 1977 to assess launch and flight behavior at minimum gyroscopic stability ($M = .98$, $\rho = 1.320 \text{ kg/m}^3$). Four of the projectiles were intentionally launched at high angles of attack (up to 11°) to determine their ability to recover from poor launch conditions. Twenty 155mm NCB-A projectiles have been launched at critical Mach numbers ($M = .98$) and at supersonic velocities[†] at Tonopah Test Range, Nevada, on 5-6 April 1977 to assess launch and flight behavior over the full range⁷. Nine of the 155mm NCB-A projectiles were launched at Tonopah Test Range on 18 October 1977

* Although 155mm projectiles can be flown in the Transonic Range, the pitching and Magnus moment are determined more accurately by using the 105mm projectiles.

† Supersonic launches were limited to $V = 625$ to 660 M/sec ($M \approx 1.8$) due to the loss in chamber volume caused by the boattail intruding into the propellant chamber. The standard 549 projectile is launched from the same gun up to $M = 2.25$.

5. Anders S. Platou, "An Improved Projectile Boattail. Part IV," ARBRL-MR-02826, April 1978, U.S. Army Ballistic Research Laboratory, Aberdeen Proving Ground, Maryland. AD B027520L.
6. John H. Whiteside, "Transonic Tests of the 155mm Non-Conical Boattail Projectile A and 8-Inch XM650E4 and EBVP Projectiles at Nicolet, Canada, During January-February 1977," ARBRL-MR-02809, January 1978, U.S. Army Ballistic Research Laboratory, Aberdeen Proving Ground, Maryland. AD B027297L.
7. Vural Oskay and Anders S. Platou, "Yawsonde Tests of 155mm M549 Non-Conical Boattail Projectile at Tonopah Test Range," ARBRL-MR-02905, March 1979, U.S. Army Ballistic Research Laboratory, Aberdeen Proving Ground, Maryland.

along with five 155mm M549 projectiles all at supersonic velocities⁸. All of the projectiles launched at Nicolet and Tonopah were instrumented with yawsonde instruments to record the projectile angular motion during each flight⁹. Radar data were also recorded so that complete velocity and trajectory information are available on each flight.

Two sizes of wind tunnel models were built of this configuration. A 2½-inch diameter model for supersonic tests ($M = 1.75$ and 2.25) at the Naval Surface Weapons Center (NSWC) and an 8-inch diameter model for transonic tests at Naval Ship Research and Development Center (NSRDC) ($M = .85$ to $.98$). The 8-inch diameter model permitted close to full scale Reynolds number testing at transonic Mach numbers (Figure 6) and the 2½-inch diameter permitted shock reflection free testing at $M = 1.75$ and 2.25 , but at low Reynolds number.

III. THE AERODYNAMIC CHARACTERISTICS

The new projectile configuration differs from conventional projectiles in four respects:

1. The three twisted "flat" surfaces used to form the boat-tail, taper the main projectile cylinder to a smaller base area such that the cross-sectional area distribution along the boattail is completely changed (Figure 7).

2. The three twisted "flat" surfaces also provide aerodynamic lifting surfaces on the rear of the projectile, which reduces the pitching moment and increases the gyroscopic stability.

3. The boattail portion of the new projectile is not axisymmetric which leads to reduced yawing forces and moments which are helpful in maintaining good flight stabilities. The asymmetry also alters the rolling moments of the projectile such that during flight the projectile spin (Pd/V) does not increase as much as for a conical boat-tailed projectile.

8. Anders S. Platou, "Yawsonde Flights of 155mm Non-Conical Boattail Projectile Configurations at Tonopah Test Range--October 1977," AHBRL-MR-02381, November 1978, U.S. Army Ballistic Research Laboratory, Aberdeen Proving Ground, Maryland. AD A065356.

9. William H. Mermagen and Wallace H. Clay, "The Design of a Second Generation Yawsonde," BRL Memorandum Report No. 2368, April 1974, U.S. Army Ballistic Research Laboratory, Aberdeen Proving Ground, Maryland. AD 780064.

4. The new boattails also provide additional wheel bearing for the projectile while it is in-bore. This should provide less muzzle jump and lower first maximum yaws. The boattail also provides a good mechanism for imparting full spin as well as forward velocity to a projectile through a discarding sabot.

To show the improved aerodynamic characteristics and flight behavior the data obtained on the non-conical boattail projectile A are summarized and compared with the standard M549 projectile in this paper.

A. Drag

The drag characteristics of this configuration are obtained from the 20mm, 105mm, and 155mm flights in the BRL Aeroballistic Ranges and the 155mm full range yawsonde instrumented flights at Tonopah. These results are presented in Figure 8. The drag of this configuration is lower than that of the conical boattailed M549 configuration over the entire Mach number range. The lower drag is due at least in part to the smaller base area of the new boattail.

$C_{D\delta^2}$ has been estimated from the BRL Aeroballistic Range flights as 3 for subsonic and transonic velocities and 4 for supersonic velocities. These values are approximate, but appear to be considerably lower than the values for the M549³ ($C_{D\delta^2} = 7$ to 9).

B. Pitching Moment

The pitching moment characteristics have been obtained from the 20mm, 105mm, and 155mm projectile flights in the BRL ranges, the wind tunnel results at NSRDC and NSWC, and the yawsonde flights at Nicolet and Tonopah. The results are summarized in Figure 9 for low angles of attack. There is good agreement of data at all Mach numbers from all sources; and it is seen that the maximum pitching moment ($C_{M\alpha} = 5.0$)

occurs at $M = .97$ to $.98$. This compares with $C_{M\alpha_{max}} = 5.5$ at $M = .94$

for the standard M549 projectile. It is also seen that the new configuration has a lower pitching moment over the entire Mach number range of interest. It should be noted here that the pitching moment of the NCB-A is lower than that of the M549 in spite of the one-half caliber additional length of the NCB-A. If the M549 were one-half caliber longer, its' maximum $C_{M\alpha}$ would be 5.5 to 6.0.

Data at higher angles of attack obtained from the wind tunnels and ranges (Figures 10 to 15) show the pitching moments on the new projectile are linear up to 5° . As with the M549, at higher angles of

attack the pitching moment slope decreases (Figures 10 to 15) so that greater gyroscopic stability is obtained.

During the wind tunnel tests of the NCB-A projectile, at transonic velocities configurations of both the straight and twisted (1/20) triangular boattail, with and without a rotating band were tested. The data (Figures 10 to 15) apply to all of these configurations when the projectile is spinning near the twist rate of the boattail. When the spin is far from the boattail twist, there is evidence at transonic speeds (Figures 16, 17, 18, and 19) that the normal force and pitching moment change with angles of attack. These data show the normal force increases and the pitching moment decreases as the spin (Pd/V) differs greatly from the boattail twist. This is probably due to partial flow separation from portions of the boattail flats when the spin differs greatly from the boattail twist. The data at supersonic speeds ($M = 1.76$ and 2.27) show the normal force and pitching moment do not change with spin at least up to angles of attack of 10° .

C. Pitch Damping Moment

The pitch damping moments on the new projectile have been obtained from the BRL Aeroballistic Range flights, using a linearized force-moment system. The data are presented in Figure 20 and indicate that the new projectile has the same pitch damping characteristics (within the accuracy of the data) as the M549. $C_{M_q} + C_{M_{\dot{\alpha}}}$ is -15 to -20 for supersonic speeds and decreases to 0 to -10 at transonic speeds.

D. Rolling Moments

Unlike conventional artillery projectiles, the new projectile has a rolling moment ($C_{\ell_{\delta_b}}$) due to the boattail twist ($\delta_b = pd/2V$) which

maintains roll rate on the projectile during flight. Therefore, measurements of roll damping (C_{ℓ_p}) and $C_{\ell_{\delta_b}}$ are needed to predict the

projectile spin. Some flight values for these coefficients have been obtained, but additional data are required. The data (Table 6) have been obtained from reduction of the yawsonde data from several of the 155mm full range flights. The reader is cautioned that these coefficients must be used together¹⁰. Use of a roll damping coefficient, C_{ℓ_p} , without the boattail-twist rolling moment, $C_{\ell_{\delta_b}}$, will result in an

erroneous spin prediction.

10. Charles H. Murphy, "Free Flight Motion of Symmetric Missiles," BRL Report No. 1216, July 1963, U.S. Army Ballistic Research Laboratory, Aberdeen Proving Ground, Maryland. AD 442757.

E. Yawing Force and Moment

Even though it is not possible to theoretically predict the yawing forces and moments on the new projectile, it is possible by using existing Magnus force and moment theories to visualize the mechanisms producing these forces and moments. On the new projectile configuration the side force and moment are a combination of two forces.

At all Mach numbers, the Magnus force developed on the front, axisymmetric portion of the new projectile is that described in reference 2. This force is in general linear with spin as shown in Figure 21 and acts in the negative direction when the projectile is at a positive angle of attack. On the boattail, however, a side force is created by the asymmetry of the boattail. The force is non-zero at zero spin and will be approximately zero when the projectile is spinning at the boattail twist. The combined side forces acting on the projectile are illustrated in Figure 22. From Figure 21, assuming the forces and moments are linear with spin, the force and moment existing on the projectile at any spin at a given angle of attack can be expressed by:

$$C_Y = C_{Y_o} + C_{N_p} \text{ pd/V}$$

$$C_n = C_{n_o} + C_{n_p} \text{ pd/V}$$

where C_{Y_o} and C_{n_o} are the zero spin offsets at each angle of attack and C_{N_p} and C_{n_p} are the Magnus force and moment spin slopes at each angle of attack.

The coefficients C_{Y_o} , C_{n_o} , C_{N_p} , and C_{n_p} have been determined from wind tunnel tests (Figures 23 and 24) at two supersonic speeds, but at low Reynolds numbers. There is a considerable difference in the offset values (C_{Y_o} and C_{n_o}) between $M = 1.76$ and 2.27 which is not readily explainable. The offsets are, most likely, Reynolds number sensitive and may change considerably at real flight conditions. The author suspects the offset values at $M = 1.76$ may be more like those observed at $M = 2.27$ at the higher free flight Reynolds numbers. To partially overcome this difference, the values of C_Y and C_n at $M = 1.76$ have been computed at $\text{pd/V} = .314$ using both sets of offset values. This is shown in Figure 25 (.314 is the twist value of the gun and the boattail used in these tests). The difference in the yawing moment is significant for it controls to a large extent the limit cycle amplitude seen in the angular motion of the projectile.

Even though the Reynolds number of the transonic wind tunnel tests on the NCB-A is correct, the tunnel turbulence and the instrumentation were such that C_{Y_0} and C_{n_0} could not be well determined. However, the indication from these transonic tests is that C_{Y_0} and C_{n_0} are much smaller than at supersonic speeds. If this is true the combined side force and moment will be less dependent on spin at transonic velocities than at supersonic velocities.

A comparison of wind tunnel results with the BRL Aeroballistic Range results shown in Figure 26 indicates that all of the measurements are of the same magnitude. Because of the nonmirror symmetries and the nonlinearities which exist in the yawing moment, comparisons between range and wind tunnel results must be made at the same spin and angle of attack levels.

Yawing moments have also been computed from the full range projectile angular motion obtained through the yawsonde instrumentation. These computations have been carried out using the procedure described in reference 11. These computations again indicate yawing moment nonlinearities with angle of attack. For the angle of attack and spin range of interest the nonlinearity can be expressed as:

$$C_{\dot{n}} = C_{n_{\alpha}} \alpha - C_{n_{\alpha^3}} \alpha^3$$

Using the values of $C_{M_q} + C_{M_{\dot{\alpha}}}$ obtained from the BRL Aeroballistic Ranges (Figure 20) and values of $C_{n_{\alpha}}$ estimated from the wind tunnel results, values of $C_{n_{\alpha^3}}$ were computed from the yawsonde data (Table 7).

F. Damping of the Epicyclic Arms

In order that the projectile angular motion remain small, or in ballistic terms remains stable, it is necessary that each arm damping rate (λ_F and λ_S) be zero or negative or if one rate is positive its values at higher angles of attack must become negative. In the latter case, the projectile angular motion has a limit cycle and the projectile will fly at a small angle of attack during part or all of its flight.

11. Robert H. Whyte, Ray C. Houghton, and Wayne H. Hathaway, "Description of Yawsonde Numerical Integration Data Reduction Computer Programs," BRL Contract Report No. 280, December 1975, U.S. Army Ballistic Research Laboratory, Aberdeen Proving Ground, Maryland. AD B010040L.

Even though the Magnus moment and pitch damping moment coefficients are not well known for the NCB-A, it is possible to roughly determine the damping rates (λ_F and λ_S) of the epicyclic arms. Using equations obtained from reference 10, the projectile physical quantities in Table 1, and the drag, normal force, and pitching moment data obtained during these experiments, the values of λ_F and λ_S can be calculated for various values of Magnus and pitch damping moment. The results are shown in Figures 27 and 28. From these figures, it can be seen that for stable projectile motion, a projectile needs as much negative pitch damping moment as possible, and the Magnus moment must be within limits which includes zero. Too positive a Magnus moment provides nutational instability while too negative a Magnus moment leads to large angle precessional limit angles.

At transonic speeds $M = .85$ to 1.0 , the free flight data (Figures 29 a, b, and c) show the NCB-A has a 4° to 7° precessional limit cycle. Since the pitch damping moment coefficient is 0 to -10 , the Magnus moment must be such as to produce the approximate damping rates shown in the inclosed cross-hatched area (Figure 27). This agrees with the Magnus moment coefficients found in The Aerodynamic Characteristics section, Yawing Force and Moment. The increase in angular motion near the end of this flight (Figure 29b) is due to the low spin at the end of the flight.

At supersonic speeds the free flight data (Figures 30 a, b, and c) show the NCB-A has a 0° to 2° precessional limit cycle. Since the pitch damping moment coefficient is -15 to -20 , the Magnus moment must be such as to produce the approximate damping rates shown in the inclosed cross-hatched area (Figure 28). Again, this agrees with the Magnus moment coefficient found in The Aerodynamic Characteristics section, Yawing Force and Moment.

Figure 29 results are typical of the transonic flights made at Tonopah, while Figure 30 results are typical of the supersonic flights made at Tonopah. The main difference in the other flights are the launch angle of attack and the size of the fast (nutational) arm at the beginning of the flight. In all cases the fast arm damped quickly to zero, leaving only the slow (precessional) arm motion. The results of all of the flights are given in references 7 and 8.

IV. FIRST MAXIMUM YAW DISPERSION

The six NCB-A projectiles flown at Nicolet and ten of the projectiles flown at Tonopah were launched at or just above the critical Mach number ($M = .97$ to $.98$) so that minimum gyroscopic stability occurs at or soon after launch. Under this condition the possibility of a projectile yawing motion increasing (unstable motion) is the greatest, especially if the first maximum yaw is large ($\alpha > 5^\circ$). On

all of these 16 transonic flights the first maximum yaw varied from 1° to 10° and the yawsonde records show that within a few seconds of flight the projectile assumed a limit cycle motion whose amplitude (5°) is controlled by the projectile's aerodynamic characteristics. Therefore, this projectile has the ability to recover from poor launch conditions.

The remaining nineteen projectiles were flown at Tonopah at supersonic launch velocities ($V \approx 650$ m/sec). The first maximum yaw of these nineteen projectiles varied from 1.8° to 8.8° due mainly to a .030" undercut of the principle boattail diameter. Again, as with the projectiles launched at transonic velocities, the projectile angular motion for all flights quickly damped to low angles and remained stable during the entire flight.

V. IMPACT DISPERSION

In order to obtain meaningful impact dispersion data on a large caliber projectile, it is necessary that the firings be conducted under rigid, controlled conditions. Some of these conditions are:

(1) The projectiles should be fired in muzzle velocity groups of 5 to 10, each projectile being launched with the same amount of propellant.

(2) All of the projectiles in each group should be fired in a short time interval (3 minutes or less between rounds) so that meteorological conditions will be constant for all of the flights in that group over the whole trajectory.

(3) All of the projectiles in each velocity group will be fired at the same muzzle velocity within close tolerances and the muzzle velocity for each round will be accurately measured to within one-third meter per second.

(4) The impact coordinates of each projectile are measured and corrected to constant muzzle velocity. This is accomplished by calculating the dependence of range on muzzle velocity using a point mass trajectory calculation. For the NCB-A projectile the muzzle velocity-range correction is 35 meters per meter/second.

During the firing of the NCB-A projectile at Tonopah these conditions were not completely met in that the time between launches had to be extended to 10 to 15 minutes. This delay was mainly due to preparation and initialization of the yawsonde for each flight. Also, in a number of the firings, the muzzle velocity variations were considerably larger than the values considered necessary for reliable dispersion data.

The only firings of the NCB-A projectile, which can be considered to be valid for dispersion data, are the ten transonic launches at Tonopah in April 1977 and seven of the nine supersonic launches at Tonopah in October 1977. (Two of these launches are unacceptable due to inaccurate muzzle velocity measurements.) The muzzle velocities, ranges and dispersion data, are given in Table 8. These dispersions are an indication that the NCB-A projectile has acceptable dispersion*. However, these values must be corroborated with additional firings made under more closely controlled conditions.

VI. CONCLUSIONS

1. The NCB-A projectile has lower drag than the M549. It is possible that the M549 conical boattail could be lengthened to give the same base area, but the increased pitching and Magnus moments would create stability problems.

2. The NCB-A projectile has an improved pitching moment (C_{M_α}) over the M549 projectile, which gives the NCB-A higher gyroscopic stability. In this case, the improved C_{M_α} due to the non-conical boattail has been used to lengthen the NCB-A projectile and potentially increase the payload capability.

3. The NCB-A projectile has smaller Magnus or yawing moments ($C_{M_{P_\alpha}}$) than the M549 at all velocities, especially at transonic velocities. This, in turn, improves the projectile flight stability.

4. The small yawing moment creates epicyclic damping rates (λ_F and λ_S) on the NCB-A which causes it to fly with a small precessional limit cycle up to 7° during most of the flights. This causes no impairment to the projectile trajectories.

5. The dispersion data obtained from the full range flights indicate that the NCB-A will have acceptable dispersion levels. However, more closely controlled dispersion firings must be carried out before good dispersion values are available.

* Acceptable dispersion for large caliber projectiles is below .3%.

REFERENCES

1. Anders S. Platou, "An Improved Projectile Boattail," BRL Memorandum Report No. 2395, July 1974, U.S. Army Ballistic Research Laboratory, Aberdeen Proving Ground, Maryland. AD 785520. Also, ADPA 1st International Symposium on Ballistics, 13-15 November 1974, Oriando, Florida.
2. Anders S. Platou and George I. T. Nielsen, "An Improved Projectile Boattail. Part II," BRL Report No. 1866, March 1976, U.S. Army Ballistic Research Laboratory, Aberdeen Proving Ground, Maryland. AD A024073.
3. R. Kline, W. R. Herrmann, and V. Oskay, "A Determination of the Aerodynamic Coefficients of the 155mm, M549 Projectile," Technical Report No. 4764, November 1974, Picatinny Arsenal, Dover, New Jersey. AD B002073L.
4. Anders S. Platou, "An Improved Projectile Boattail. Part III," BRL Memorandum Report No. 2644, July 1976, U.S. Army Ballistic Research Laboratory, Aberdeen Proving Ground, Maryland. AD B012781L.
5. Anders S. Platou, "An Improved Projectile Boattail. Part IV," ARBRL-MR-02826, April 1978, U.S. Army Ballistic Research Laboratory, Aberdeen Proving Ground, Maryland. AD B027520L.
6. John H. Whiteside, "Transonic Tests of the 155mm Non-Conical Boat-tail Projectile A and 8-Inch XM650E4 and EBVP Projectiles at Nicolet, Canada, During January-February 1977," ARBRL-MR-02809, January 1978, U.S. Army Ballistic Research Laboratory, Aberdeen Proving Ground, Maryland. AD B027297L.
7. Vural Oskay and Anders S. Platou, "Yawsonde Tests of 155mm M549 Non-Conical Boattail Projectile at Tonopah Test Range," ARBRL-MR-02905, March 1979, U.S. Army Ballistic Research Laboratory, Aberdeen Proving Ground, Maryland.
8. Anders S. Platou, "Yawsonde Flights of 155mm Non-Conical Boattail Projectile Configurations at Tonopah Test Range--October 1977," ARBRL-MR-02881, November 1978, U.S. Army Ballistic Research Laboratory, Aberdeen Proving Ground, Maryland. AD A065356.
9. William H. Mermagen and Wallace H. Clay, "The Design of a Second Generation Yawsonde," BRL Memorandum Report No. 2368, April 1974, U.S. Army Ballistic Research Laboratory, Aberdeen Proving Ground, Maryland. AD 780064.

REFERENCES (Continued)

10. Charles H. Murphy, "Free Flight Motion of Symmetric Missiles," BRL Report No. 1216, July 1963, U.S. Army Ballistic Research Laboratory, Aberdeen Proving Ground, Maryland. AD 442757.
11. Robert H. Whyte, Ray C. Houghton, and Wayne H. Hathaway, "Description of Yawsonde Numerical Integration Data Reduction Computer Programs," BRL Contract Report No. 280 December 1975, U.S. Army Ballistic Research Laboratory, Aberdeen Proving Ground, Maryland. AD B010040L.

Table 1. Physical Characteristics of the Various Projectiles

	105mm		155mm	
	M549	NCB-A	M549	NCB-A Tonopah Nicolet
W	14.1	14.1	43.5	43.7
C.G.	3.5	3.5	3.5	3.4
Length	5.7	6.2	5.7	6.2
I_x	.022	.020	.15	.14
I_y	.224	.241	1.93	1.69

Table 2. Aerodynamic Parameters of the 105mm NCB-A Projectile With a 1/20 Caliber Twisted Triangular Boattail

Rd. No.	Mach (1)	$\bar{\alpha}_t$ degs.	C_{D_0} (3)	C_{M_α} (2)	C_{N_α}	$C_{M_{P_\alpha}}$ (2)	$C_{M_q} + C_{M_{\dot{\alpha}}}$ (2)	C.P.N Cal. Fwd. of Base
12852	.816	1.65	.1137	4.2				4.87
12860	.912	3.42	.1495	4.335	2.01	-.392	- 4.41	4.79
12868	.927	3.61	.1600	4.370	2.10	-.177	- 8.04	4.79
12863	.941	5.50	.1496	4.333	2.08	-.009	- 7.46	4.79
12855	.942	2.69	.1545	4.536	1.71	-.410	- 5.74	5.36
12857	.942	1.77	.1585	4.404	1.94	-.408	- 1.96	4.98
12866	.944	3.98	.1552	4.426	2.03	-.090	- 8.01	4.89
13085	.973	2.89	.1762	5.006	1.51	-.311	- 7.74	6.02
12871	.974	4.05	.1730	4.882	1.91	+.035	-10.60	5.27
13088	.985	3.48	.2376	4.911	2.07	+.062	-10.95	5.08
13430	.987	3.23	.2576	4.831	2.27	+.040	-10.30	4.83
13087	.989	3.23	.2655	4.791	2.36	+.103	- 9.95	4.74
13429	.995	4.86	.2816	4.471	2.43	+.352	-12.20	4.55
13427	.998	2.07	.2889	4.731	2.38	-.432	- 1.28	4.70
13428	1.004	.65	.2980	4.557	2.61	+.121	-19.50	4.46
13086	1.006	5.95	.3140	4.283	2.38	+.369	-13.00	4.51
12847	1.187	2.01	.3028	3.984	1.87	+.208	-18.80	4.84

(1), (2), (3) see footnotes Table 3.

Table 3. Aerodynamic Parameters of the 155mm NCB-A Projectile With a 1/20 Caliber Twisted Triangular Boattail

Rd. No.	Mach (1)	$\bar{\alpha}_t$ degs.	C_{D_0} (3)	C_{M_α} (2)	C_{N_α}	$C_{M_{P_\alpha}}$ (2)	$C_{M_q} + C_{M_{\dot{\alpha}}}$ (2)	C.P.N Cal. Fwd. of Base
13092	.892	3.34	.1114	4.264	1.74	-.440	- 4.0	5.1
13091	.897	3.11	.1120	4.270	2.10	-.664	- .3	4.7
13096	.920	4.97	.1250	4.288	1.94	-.050	-10.1	4.9
13093	.925	7.33	.1198	4.252	2.01	-.038	- 7.3	4.8
13420	.938	3.36	.1214	4.203	1.14	-.944	+ .2	6.4
13099	.957	5.37	.1317	4.541	1.70	-.173	- 7.2	5.4
13098	.959	2.51	.1302	4.593	2.19	-.432	-11.1	4.8
13100	1.156	7.88	.3104	3.826	2.61	+.173	-16.0	4.2
13422	1.289	10.45	.3013	3.472	3.75	+.555	-22.6	3.6
13421	1.546	4.94	.2793	3.635	2.52	-.150	- 9.7	4.1
13425	1.867	1.61	.2455	3.388	2.90	-.121	-18.5	3.8

24

(1) Mid range values

(2) All moments are about C.G. = 3.5 calibers aft of nose

(3) $C_{D_0} = C_{D_0} - C_{D_{\delta^2}}$ $\frac{\pi \bar{\alpha}_t^2}{180}$ $M < 1.2$ $C_{D_{\delta^2}} = 3$ $M > 1.2$ $C_{D_{\delta^2}} = 4$

Table 4. Aeroballistic Parameters of the 105mm NCB-A Projectile With a
1/20 Caliber Twisted Triangular Boattail and Pd/V = .314

Rd. No.	<u>S</u> g	<u>S_d</u>	$\lambda_F \times 10^{-3}$ 1/cal	$\lambda_S \times 10^{-3}$ 1/cal	<u>K_F</u> Rad	<u>K_S</u> Rad	ϕ_F Rad/Cal	ϕ_S Rad/Cal
12852	1.60				.0107	.0257	.0218	.0050
12860	1.51	- .51	-.334	+ .1420	.0301	.0512	.0207	.0054
12868	1.51	+ .16	-.347	+ .0537	.0395	.0494	.0206	.0054
12863	1.51	+ .55	-.245	-.0380	.0608	.0742	.0208	.0055
12855	1.45	- .62	-.407	+ .1820	.0206	.0418	.0204	.0058
12857	1.50	- .92	-.298	+ .1500	.0075	.0299	.0201	.0077
12866	1.48	+ .34	-.312	+ .0157	.0398	.0567	.0205	.0056
13085	1.32	- .34	+ .507	+ .1370	.0284	.0409	.0198	.0065
12871	1.35	+ .47	-.391	-.0486	.0438	.0549	.0198	.0063
13088	1.39	+ .53	-.272	+ .0318	.0372	.0483	.0201	.0062
13430	1.42	.54	-.272	+ .0400	.0348	.0445	.0203	.0060
13087	1.40	+ .69	-.210	-.0147	.0352	.0439	.0204	.0060
13429	1.54	.98	-.181	-.1619	.0642	.0612	.0210	.0054
13427	1.44	- .89	-.240	+ .1017	.0170	.0316	.0206	.0058
13428	1.50	+ .44	-.587	+ .1093	.0042	.0106	.0206	.0056
13086	1.61	+1.00	-.201	-.1870	.0635	.0820	.0215	.0051
12847	1.59	+ .47	-.538	-.0253	.0158	.0311	.0210	.0050

Table 5. Aeroballistic Parameters of the 155mm MCB-A Projectile With
a 1/20 Caliber Twisted Triangular Boattail and Pd/V = .314

Rd. No.	S_g	S_d	$\lambda_F \times 10^{-3}$ 1/cal	$\lambda_S \times 10^{-3}$ 1/Cal	K_F Rad	K_S Rad	ϕ_F Rad/Cal	ϕ_S Rad/Cal
13092	1.30	-.96	-.383	+.2470	.0224	.0534	.0177	.00612
13091	1.29	-.31	-.471	+.3390	.0225	.0487	.0176	.00623
13096	1.31	+.36	-.353	+.0383	.0460	.0742	.0179	.00616
13093	1.34	+.50	-.293	-.0049	.0773	.1021	.0182	.00597
13420	1.37	-15.7	-.395	+.5930	.0296	.0493	.0177	.00594
13099	1.23	.06	-.444	+.0561	.0534	.0769	.0174	.00661
13098	1.24	-.31	-.776	+.3530	.0179	.0393	.0170	.00688
13100	1.51	.61	-.416	-.0930	.0832	.1090	.0193	.00505
13422	1.56	.93	-.359	-.2660	.1324	.1248	.0185	.00463
13421	1.56	.26	-.416	+.0129	.0537	.0680	.0189	.00473
13425	1.20	.25	-.629	+.0140	.0129	.0252	.0195	.00436

Table 6. Rolling Moment Coefficients of the NCB-A

M	.70	.72	.81	.92	1.27	1.46
C_{l_p}	-.125	-.101	-.075	-.037	-.096	-.083
$C_{l_{\delta_b}}$.042	.032	.022	.009	.029	.024

Table 7. Aerodynamic Data Obtained from Yawsonde Records

M	90 to .95	1.74 to 1.80
α	4.5° to 6°	2.5 to 3.2
C_{M_α}	4.38 to 4.58	3.500
$C_{M_q} + C_{M_{\dot{\alpha}}}$	-10	-20
C_{n_α}	-.4	-.4
$C_{n_{\alpha^3}}$	-.4 to 7.5	1 to 156

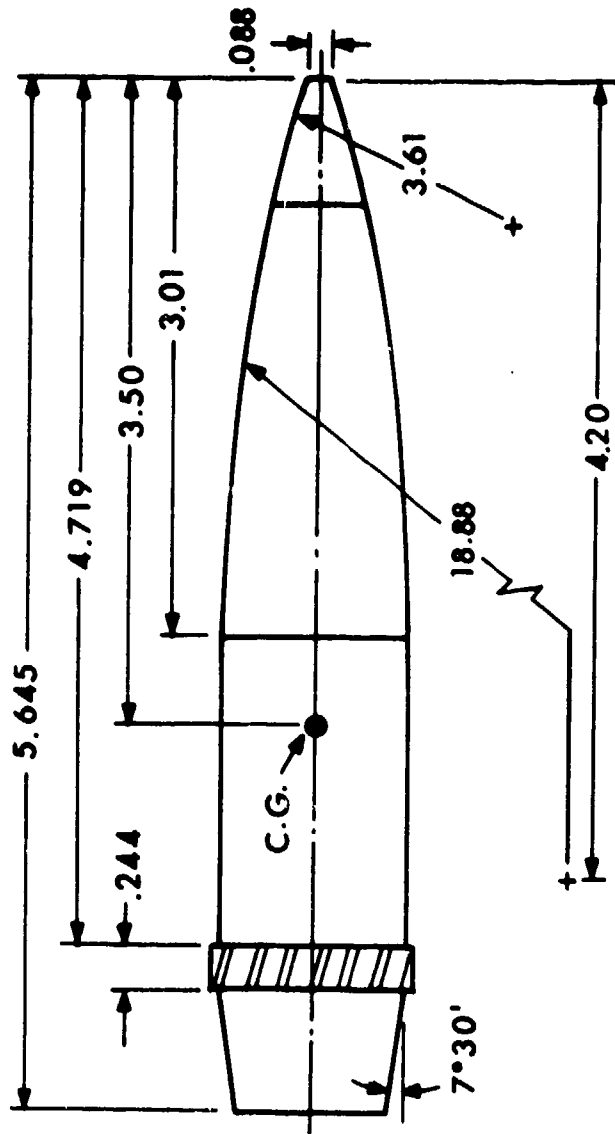
Table 8. The Impact Data from the NCB-A

<u>Round</u>	<u>Range</u> m	<u>Deflection</u> to Right m	<u>Muzzle</u> Velocity m/sec	<u>Range Corrected</u> to V = 650 m/sec m	<u>Dispersion</u>
<u>Transonic Flights</u>					
422266-05	9,291	186.0		9,491	
-06	9,252	188.8		9,463	
-07	9,402	160.6		9,515	
-08	9,361	170.7		9,505	
-09	9,382	160.8		9,528	
-10	9,427	167.0		9,566	
-11	9,660	182.6		9,660	
-12	9,469	168.9		9,540	
-13	9,471	162.6		9,540	
-14	9,574	166.1		9,623	
Average Range 9,543.1 m Standard Deviation = 59.8 m P.E. = .42%					
<u>Supersonic Flights</u>					
422276-1	20,137.5	383.1	642.3	20,388	
-2	20,467.6	337.8	651.0-659.3*	20,151	
-3	20,411.1	284.9	648.3	20,461	
-4	20,296.5	311.3	645.6	20,435	
-5	20,337.0	320.6	646.2	20,461	
-6	20,306.5	350.0	644.3	20,492	
Without Rounds 2 and 7 Average Range 20,444.3 m Standard Deviation = 35.3 m P.E. = .12%					

Table 8. Concluded

<u>Round</u>	<u>Range</u> m	<u>Deflection</u> to Right m	<u>Muzzle</u> Velocity m/sec	<u>Range Corrected</u> to V = 650 m/sec m	<u>Dispersion</u>
422276-7	20,386.4	345.0	644.8- <u>648.7</u> *	20,423	
-8	20,212.9	322.3	643.8	20,414	
-9	20,250.0	303.4	642.9	20,480	

* Velocimeter data questionable--either velocity is possible--underlined velocities maintain P.E. = .12%.



ALL DIMENSIONS IN CALIBERS
 1 caliber = 154.7 mm

Figure 1. The 155mm M549 Projectile

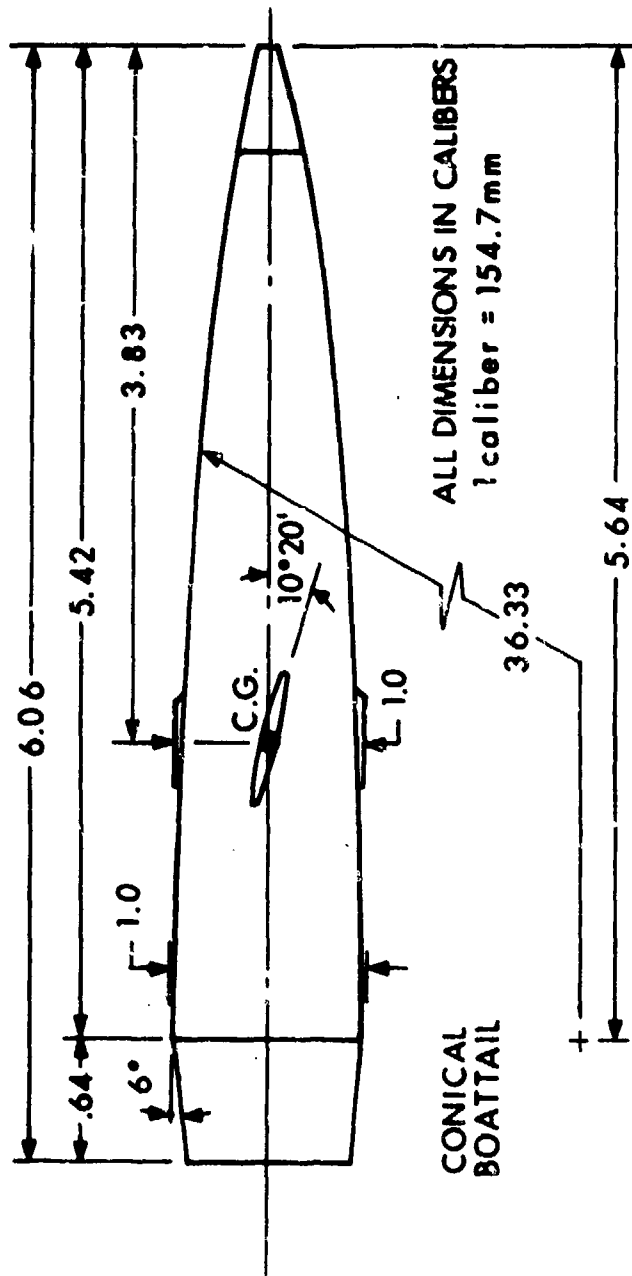


Figure 2. The 155mm SRC Projectile

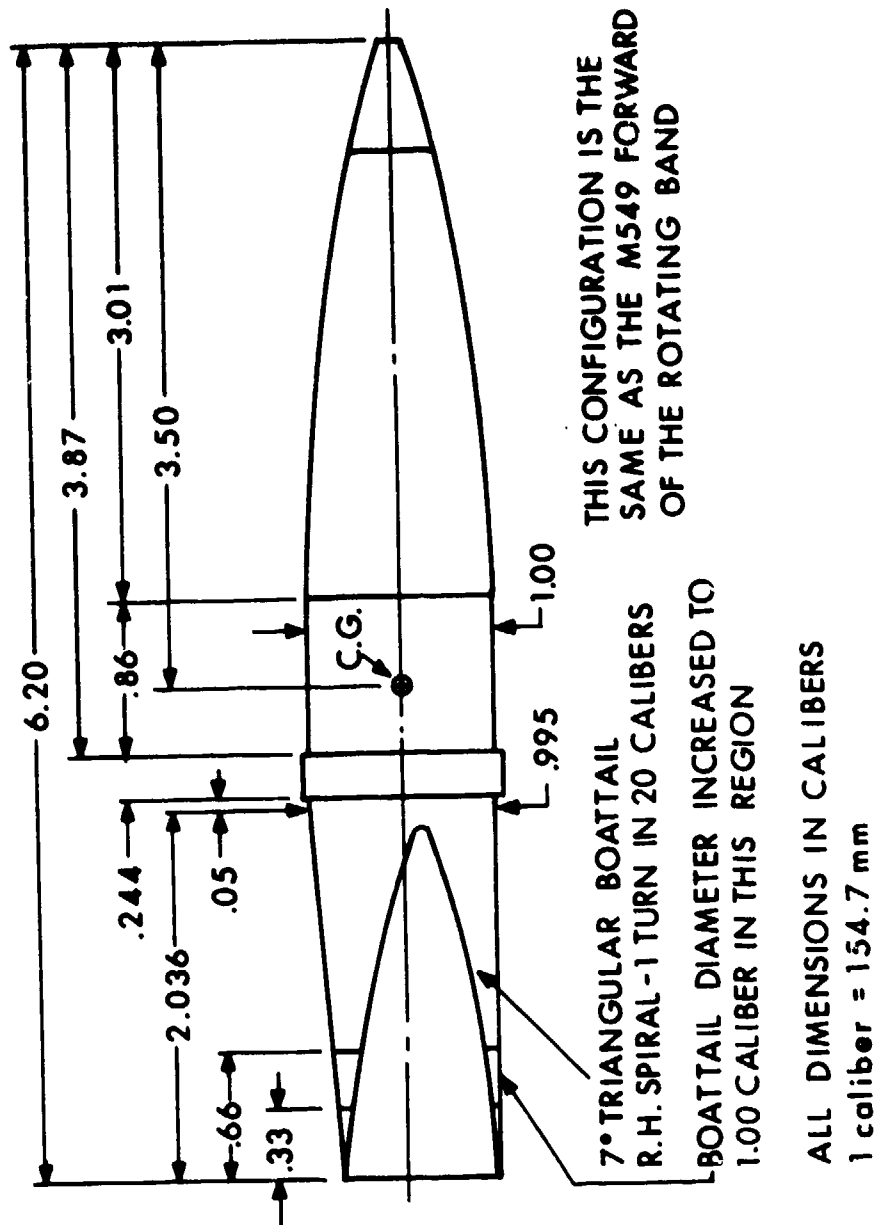


Figure 3. The 155mm Non-Conical Boattail Projectile-A (NCB-A)

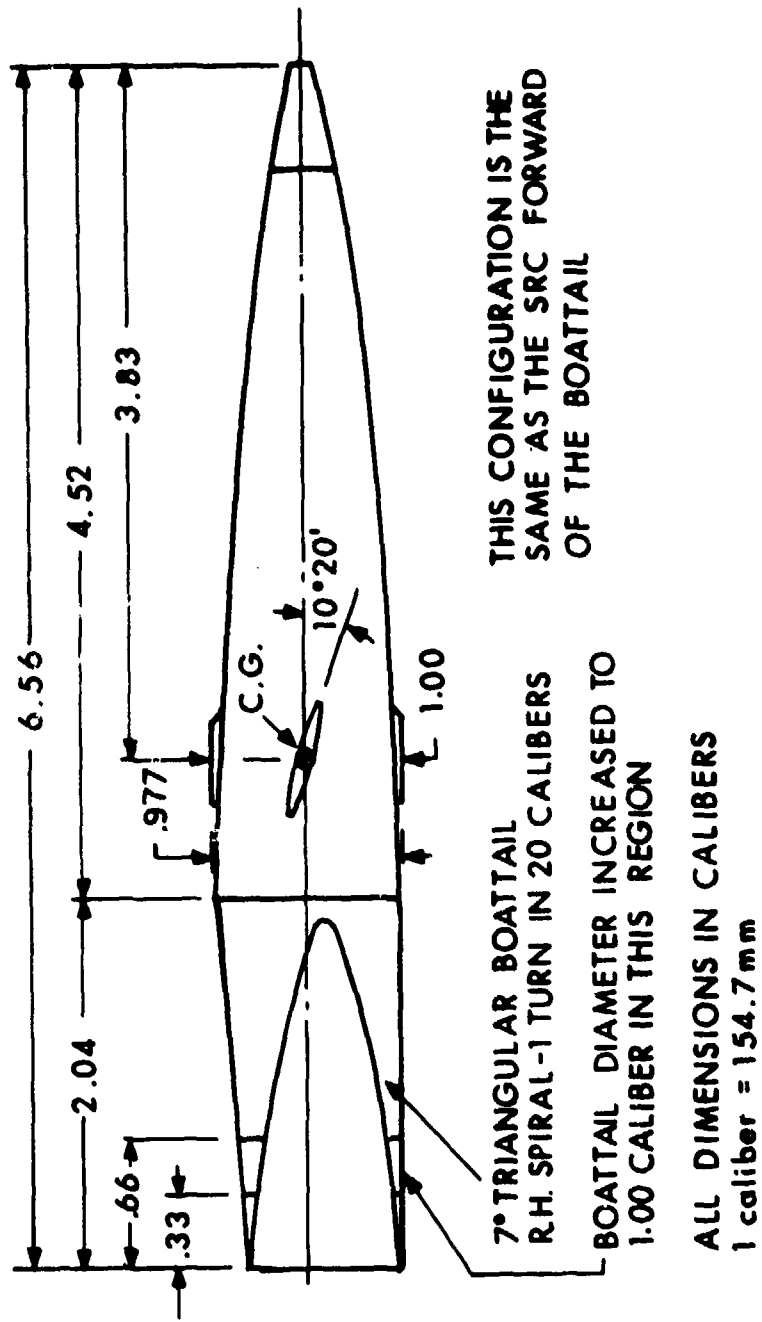


Figure 4. The 155mm Non-Conical Boattail Projectile-B (NCB-B)

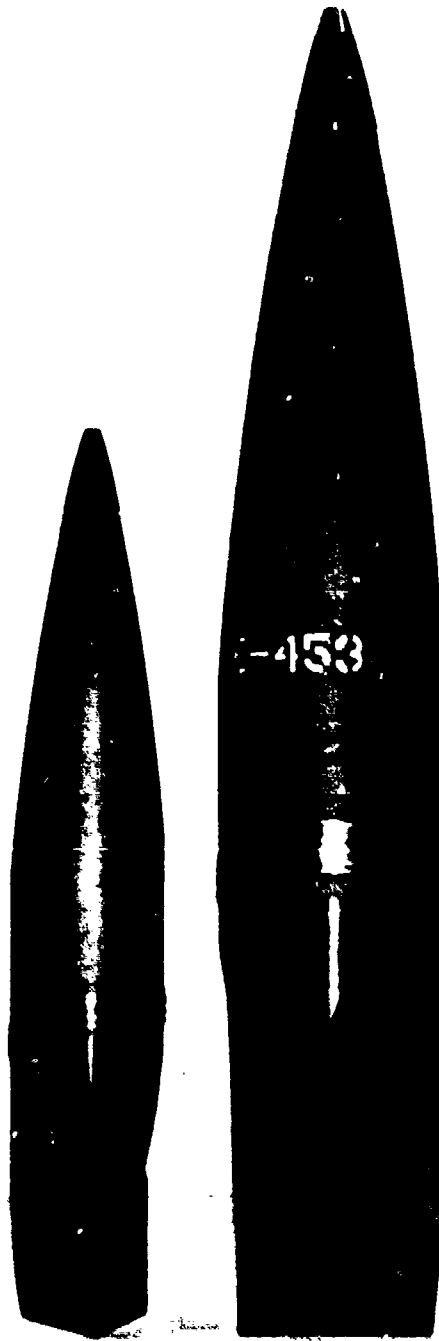


Figure 5. The 105mm and 155mm Models of the Non-Conical Boattail Projectile-A (NCB-A)

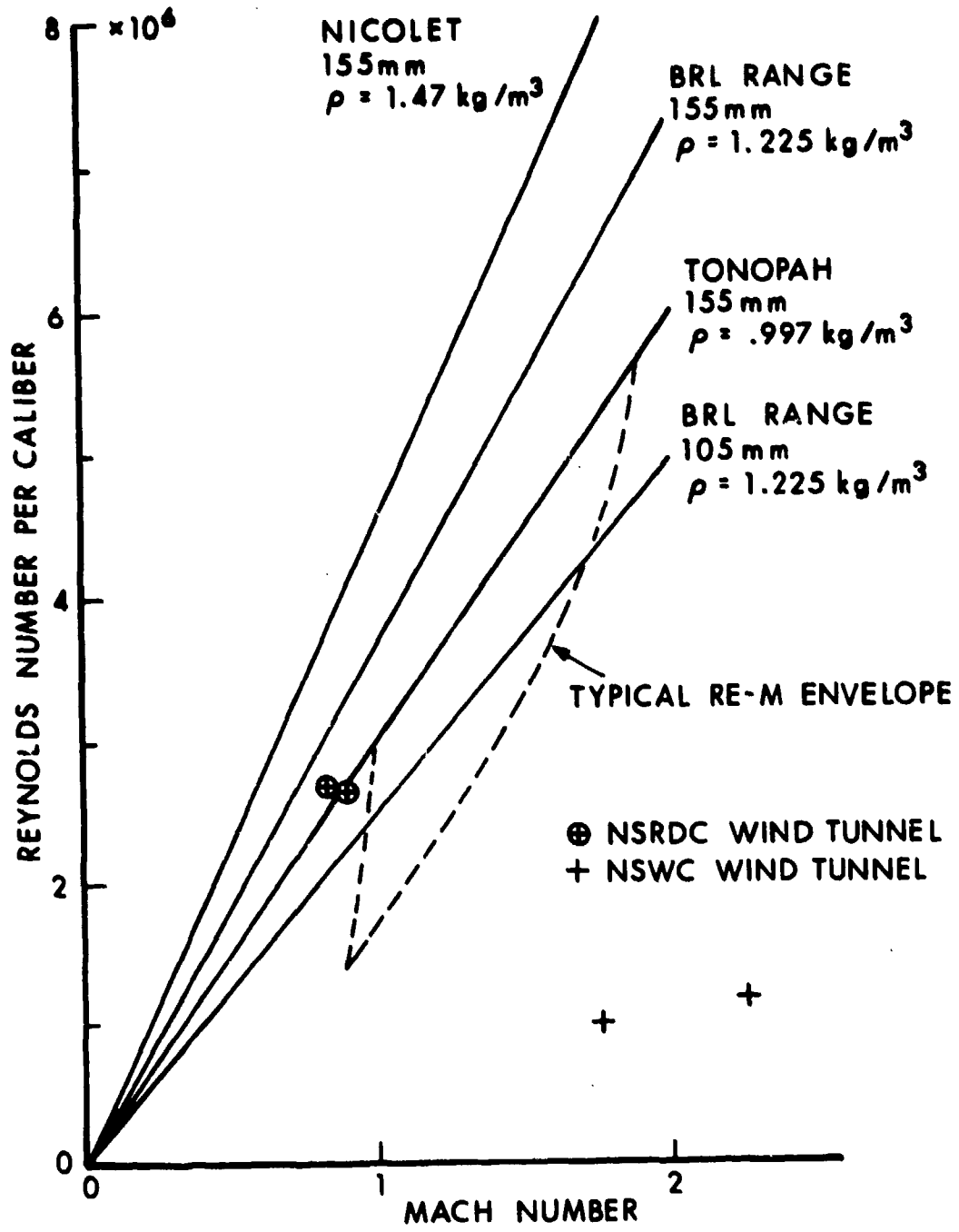


Figure 6. Free Flight and Ground Test Facilities Reynolds Numbers

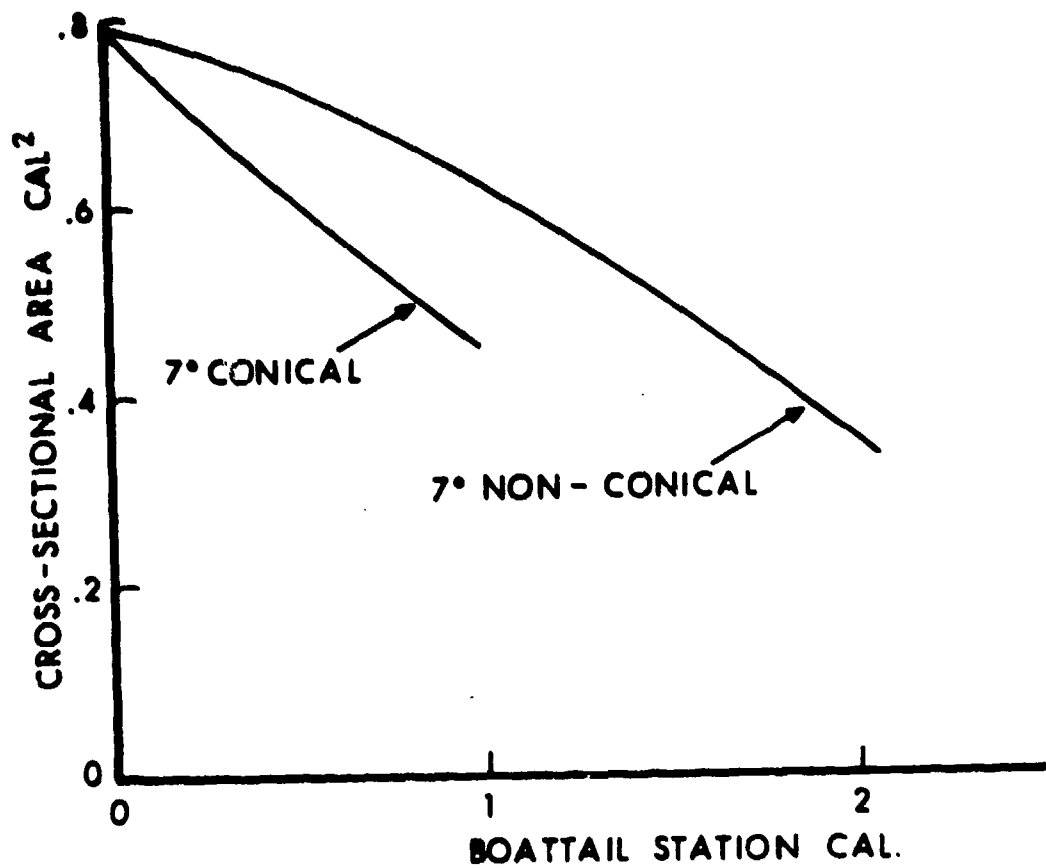


Figure 7. The Cross-Section Area Distribution of a Conical and Non-Conical Boattail

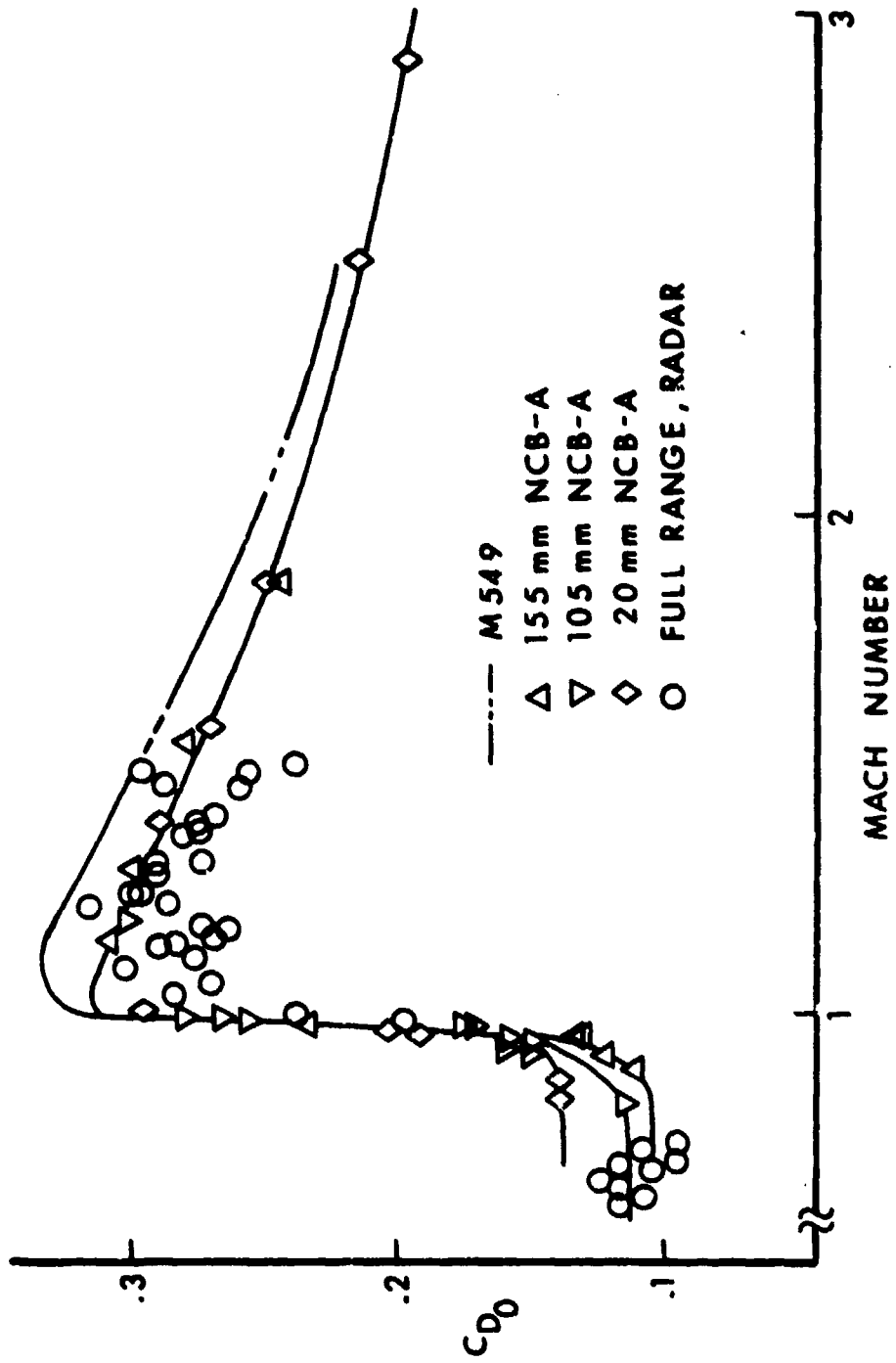


Figure 8. The Zero Yaw Drag Coefficient of the NCB-A and M549 Projectiles

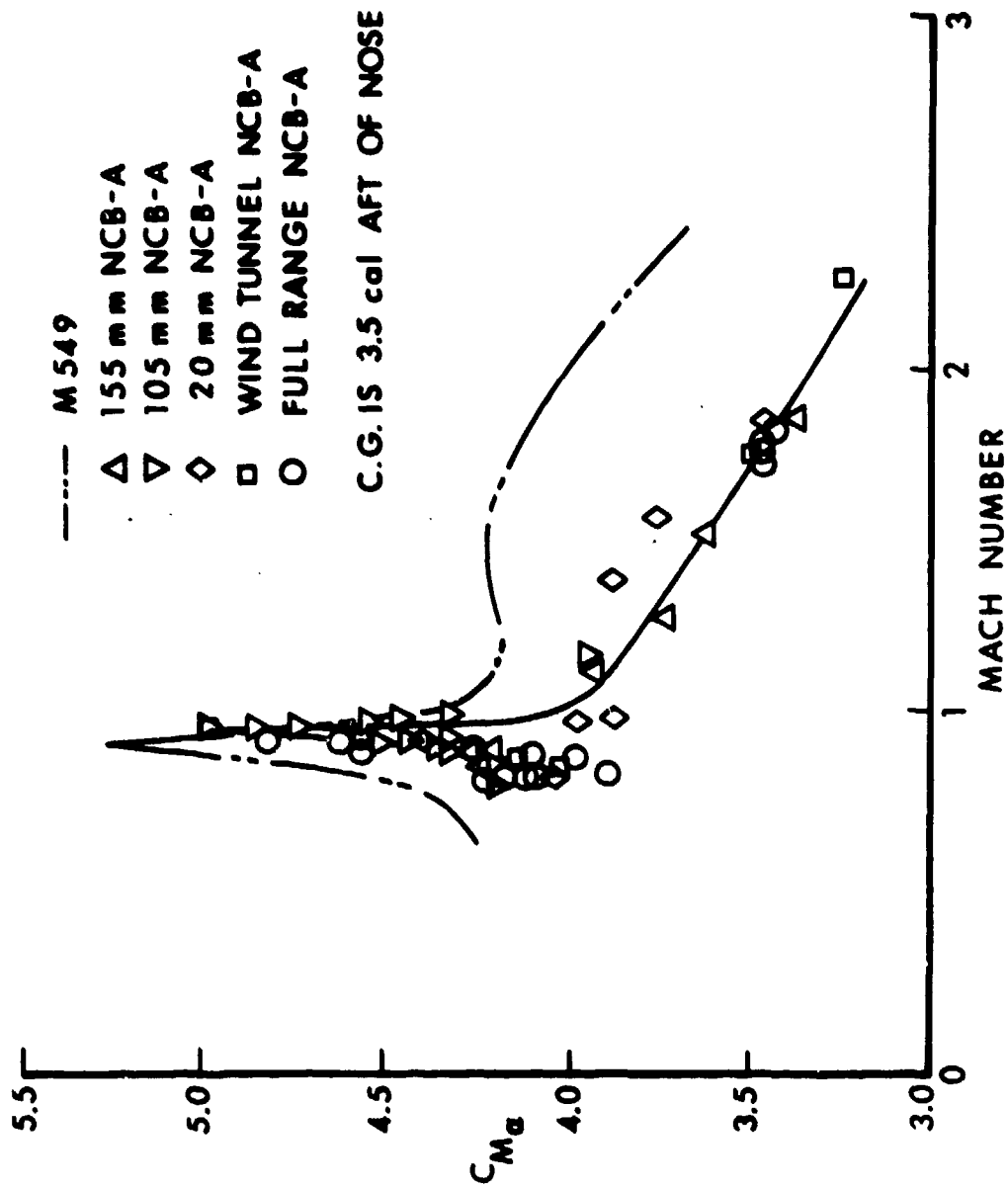


Figure 9. The Low Yaw Pitching Moment Coefficients of the NCB-A and M549 Projectiles

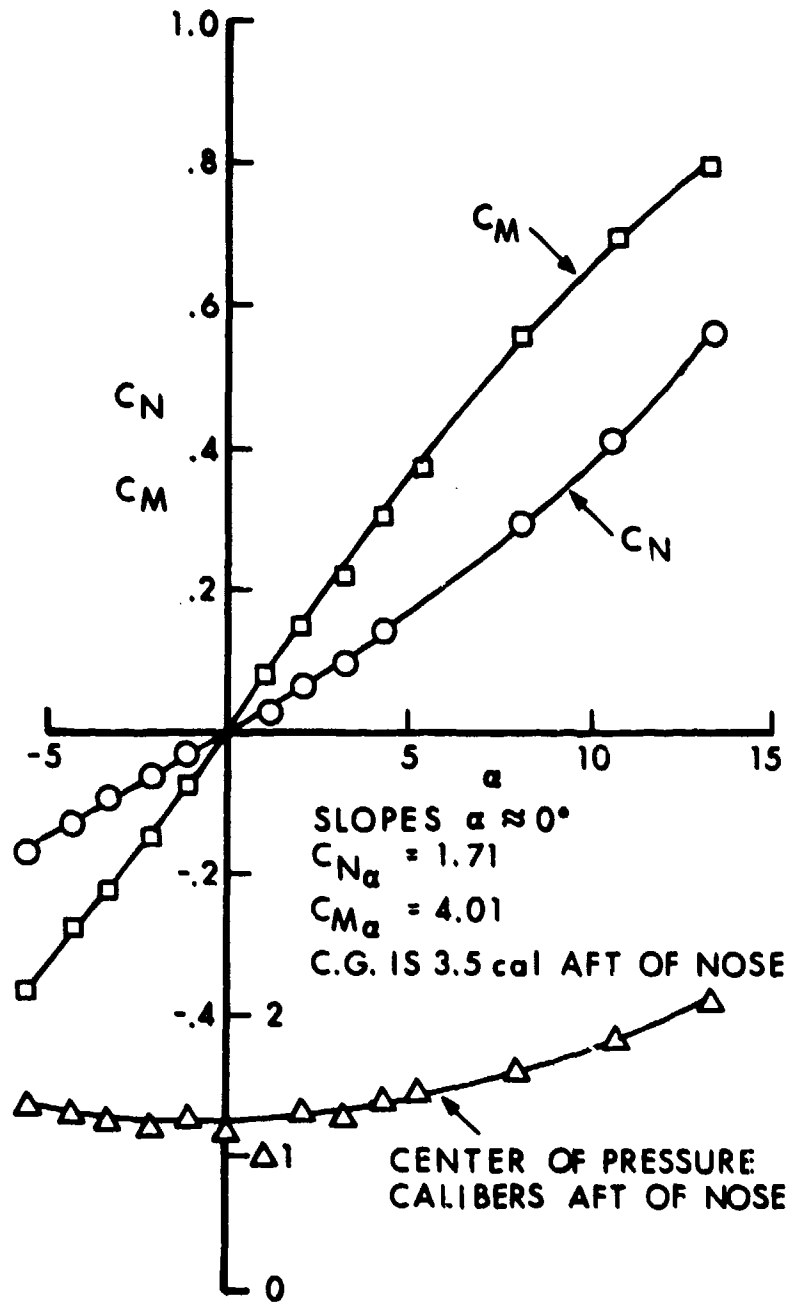


Figure 10. The Polar Characteristics of the NCB-A at $M = .851$, $R_d = 2.59 \times 10^6$

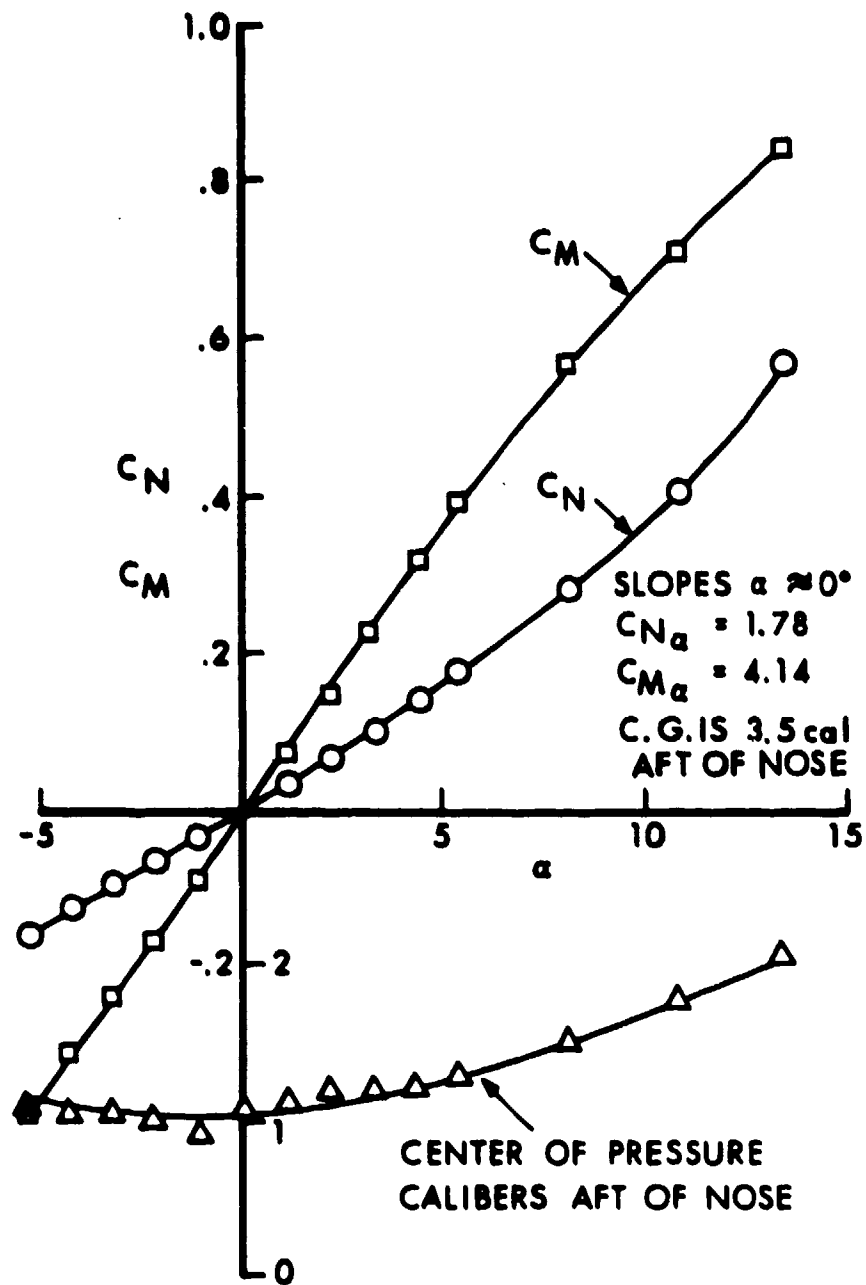


Figure 11. The Polar Characteristics of the NCB-A at $M = .90$, $R_d = 2.50 \times 10^6$

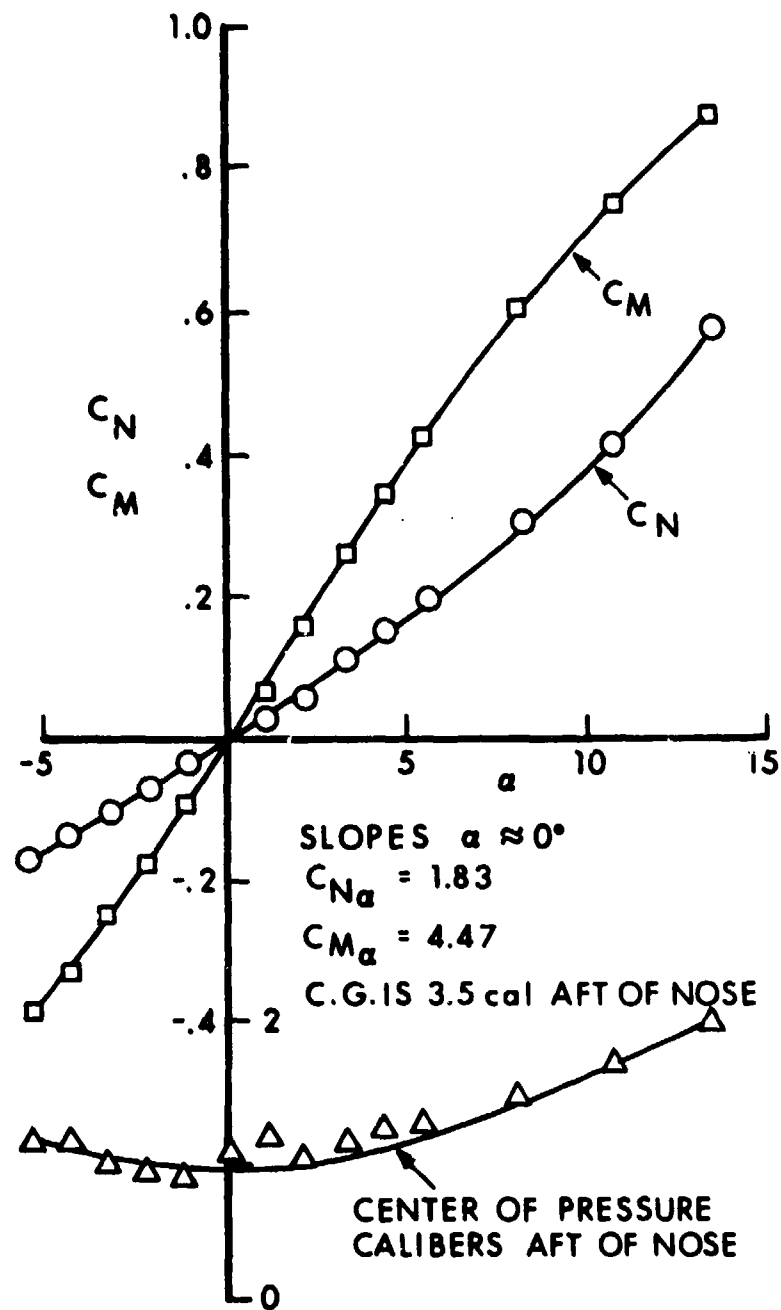


Figure 12. The Polar Characteristics of the NCB-A at $M = .951$, $R_d = 2.47 \times 10^6$

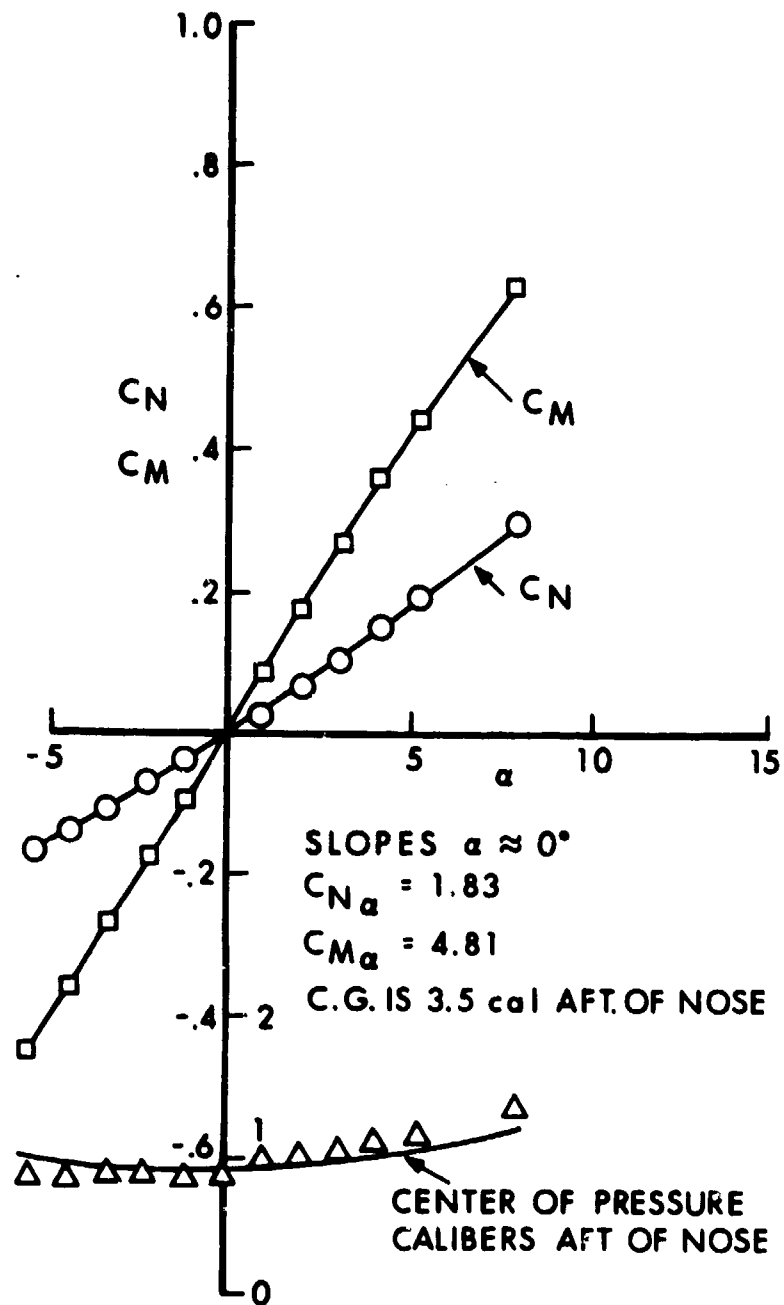


Figure 13. The Polar Characteristics of the NCB-A at $M = .978$, $R_d = 2.03 \times 10^6$

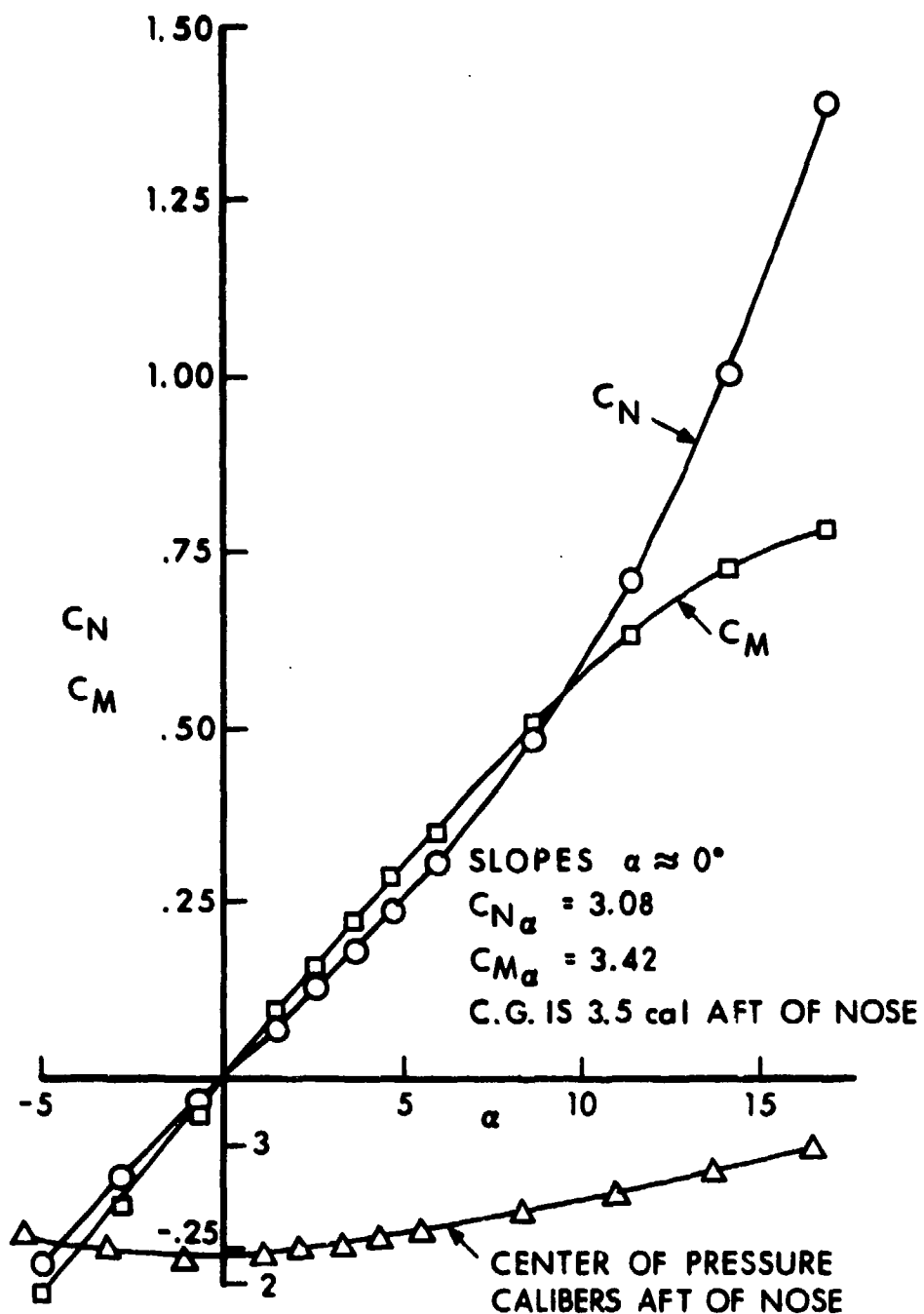


Figure 14. The Polar Characteristics of the NCB-A at $M = 1.76$, $R_d = .97 \times 10^6$

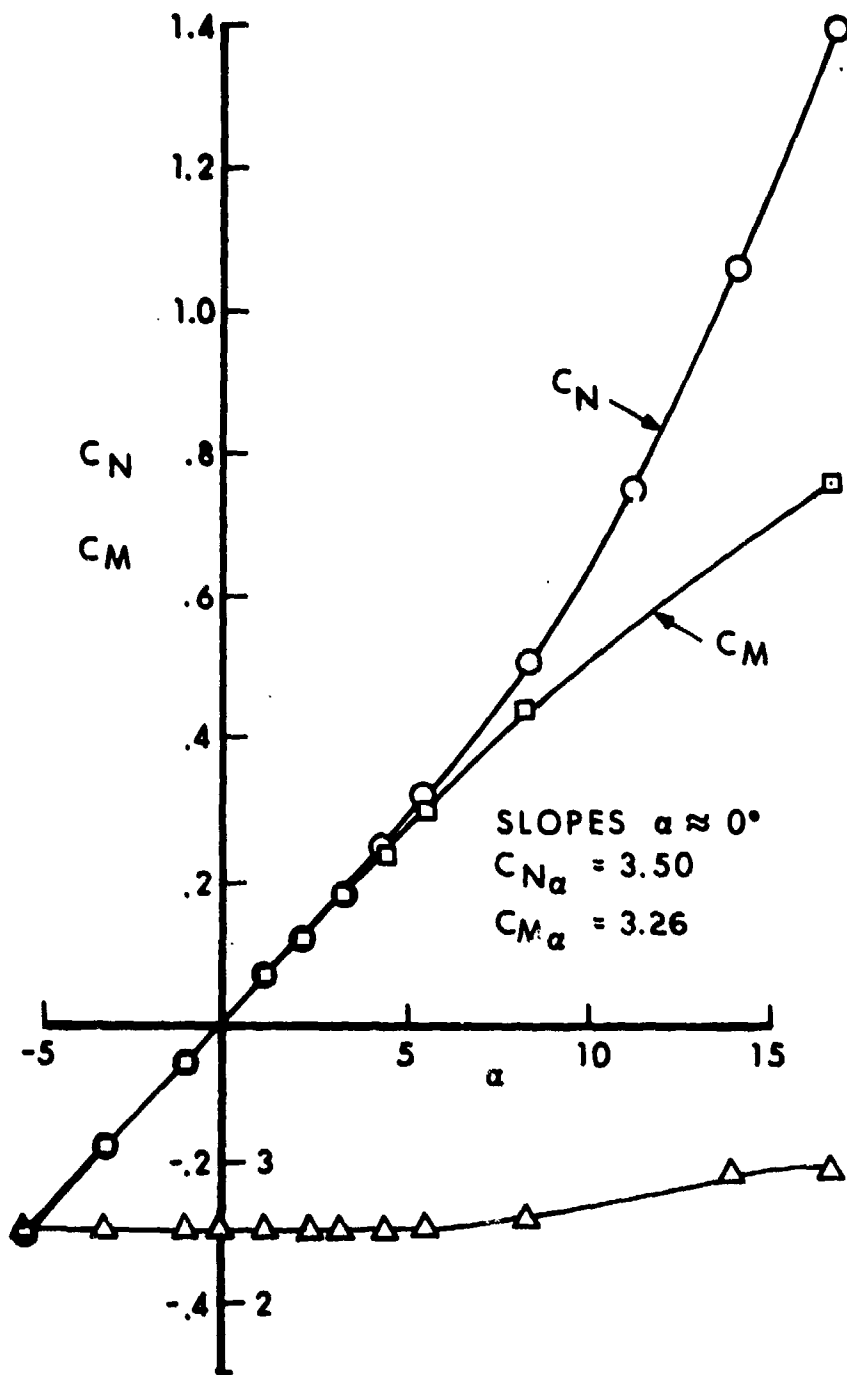


Figure 15. The Polar Characteristics of the NCB-A at $M = 2.27$, $R_d = 1.06 \times 10^6$

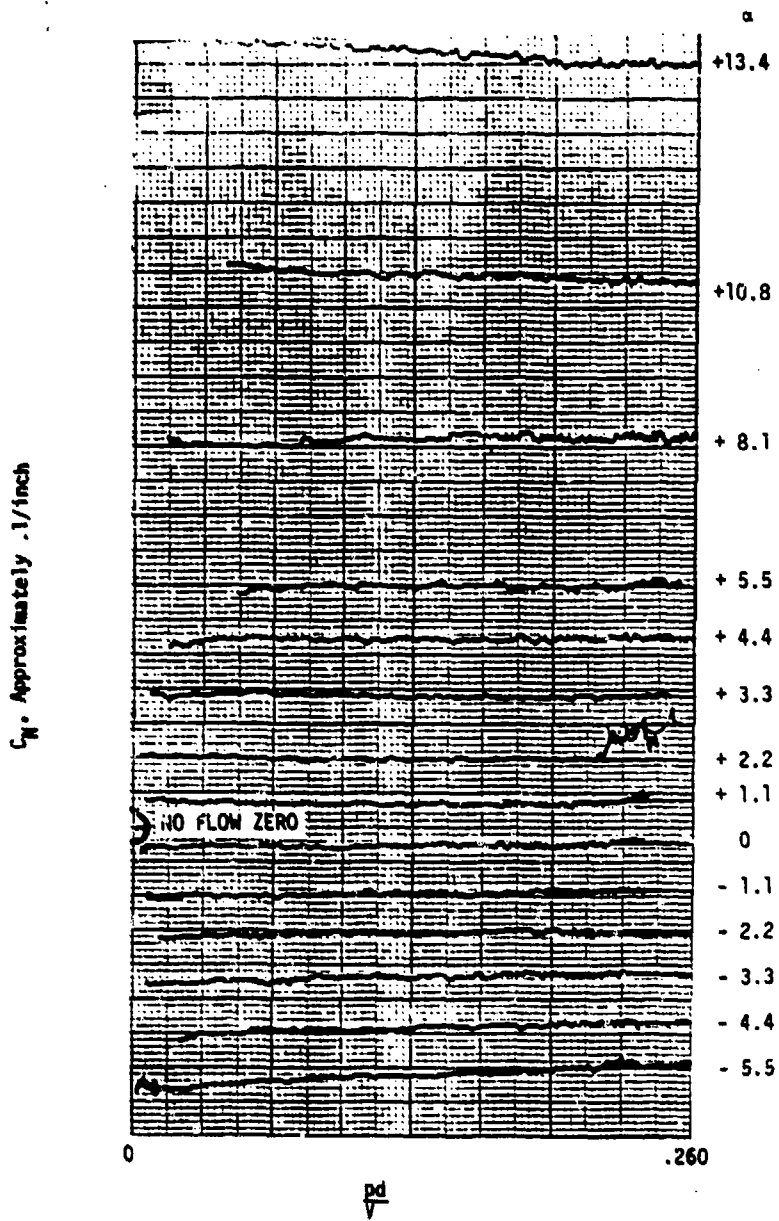


Figure 16. The Variation in Normal Force Coefficient With Spin on the NCB-A With a 1/20 Caliber Twist Boattail at $M = .95$

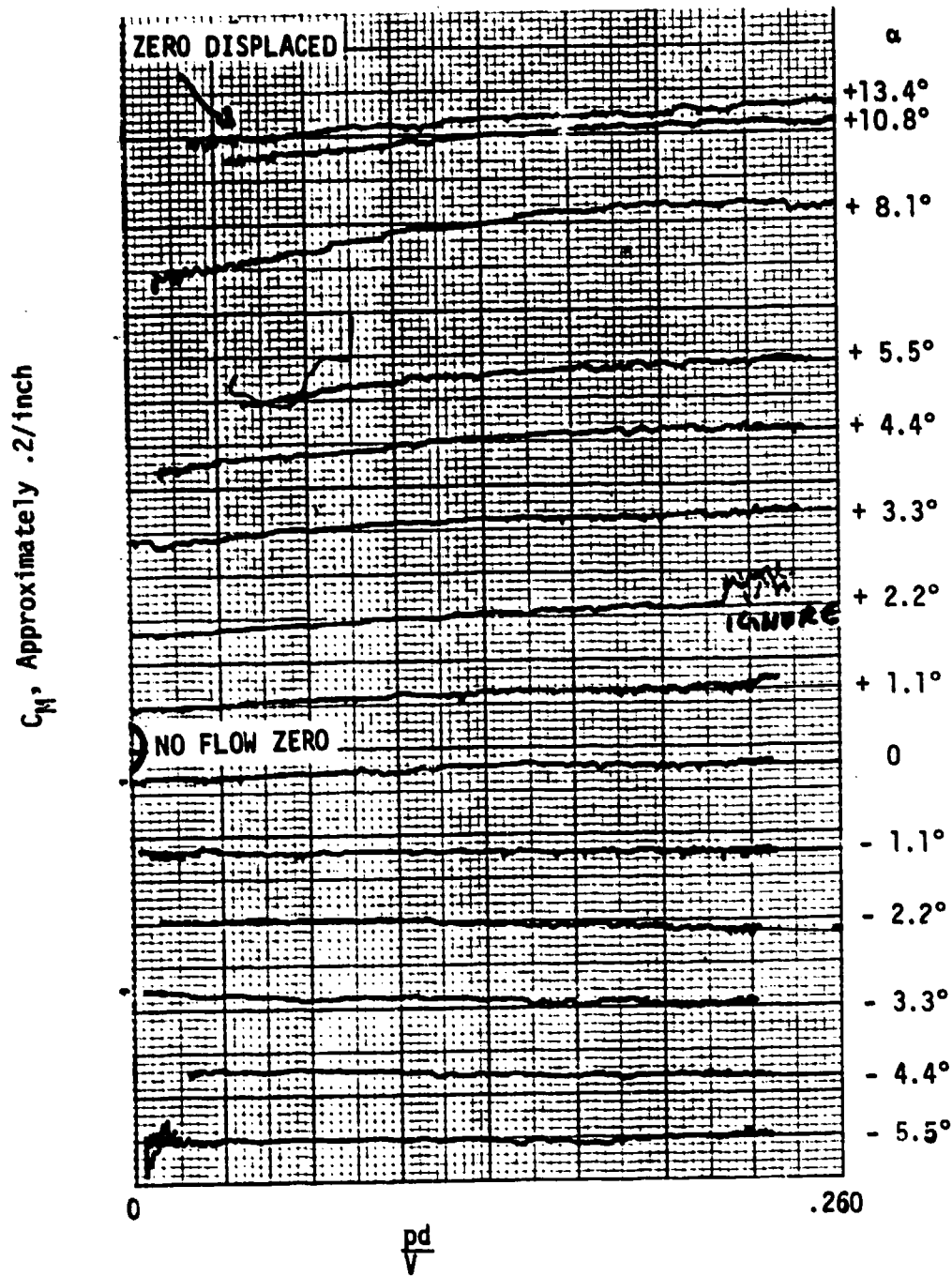


Figure 17. The Variation in Pitching Moment Coefficient With Spin on the NCB-A With a 1/20 Caliber Twist Boattail at M = .95

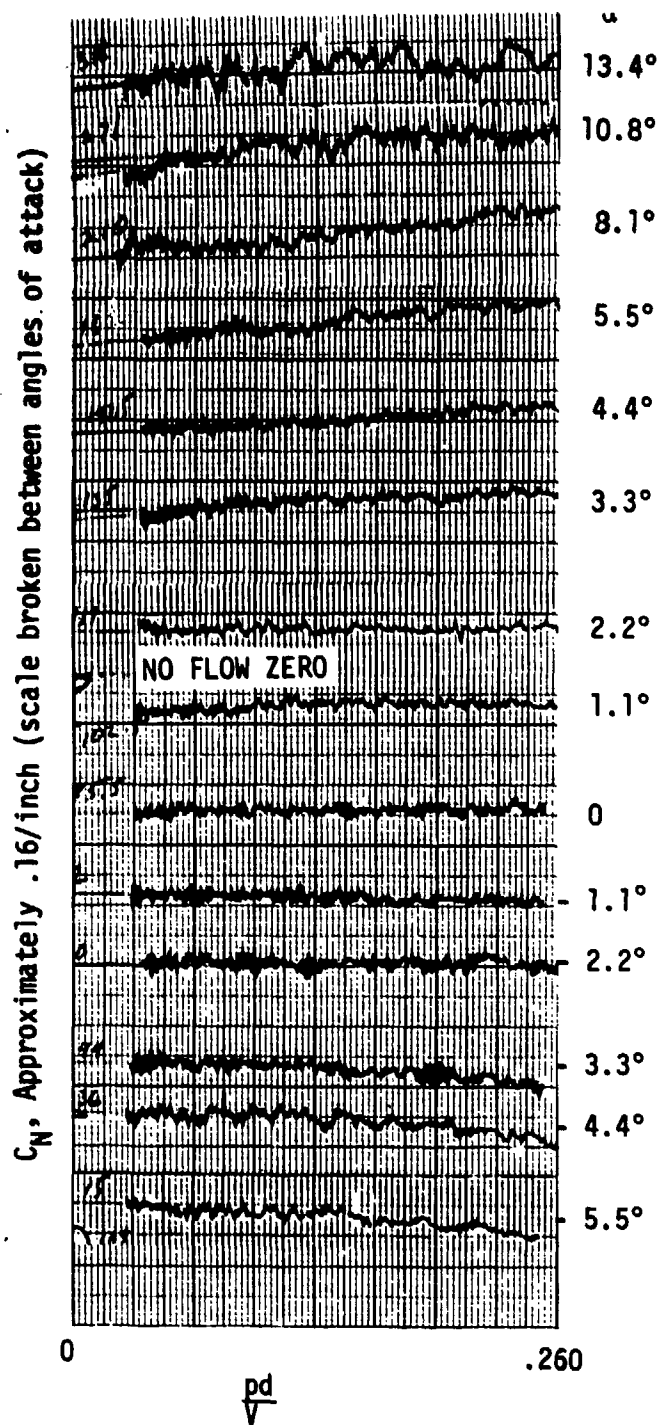


Figure 18. The Variation of the Normal Force Coefficient With Spin on the NCB-A With a Straight Boattail at $M = .95$

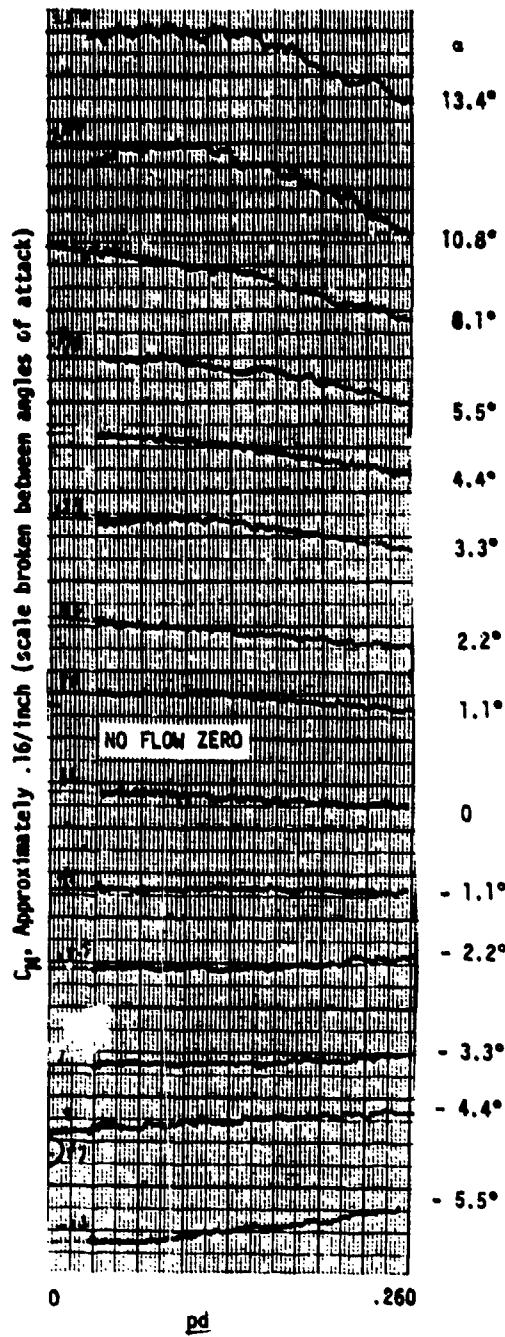


Figure 19. The Variation of the Pitching Moment Coefficient With Spin on the NCB-A With a Straight Boattail at M = .95

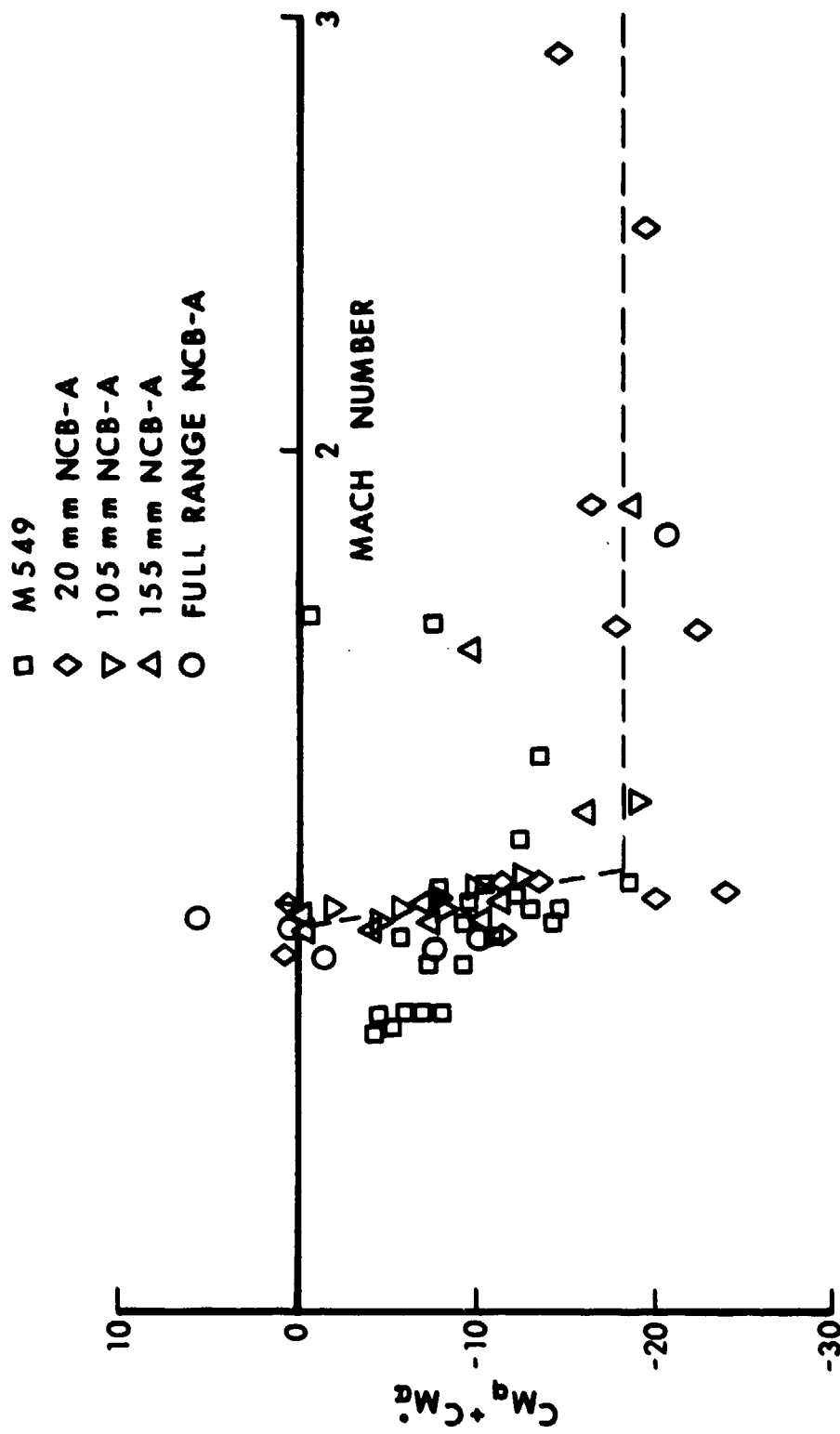


Figure 20. The Pitch Damping Moment Coefficient of the NCB-A Compared to the M549 at Small Angles of Attack, $pd/V = .314$

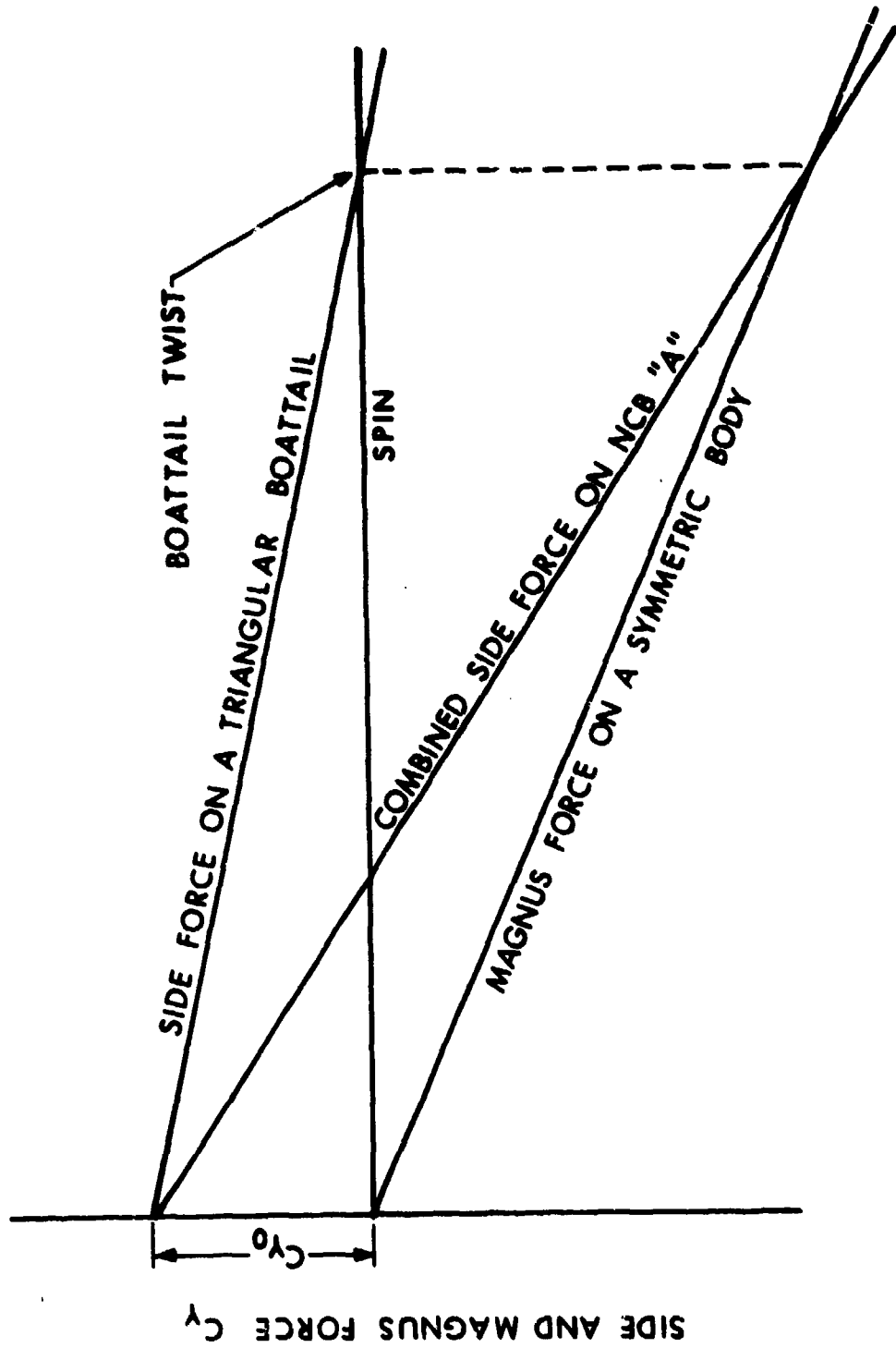
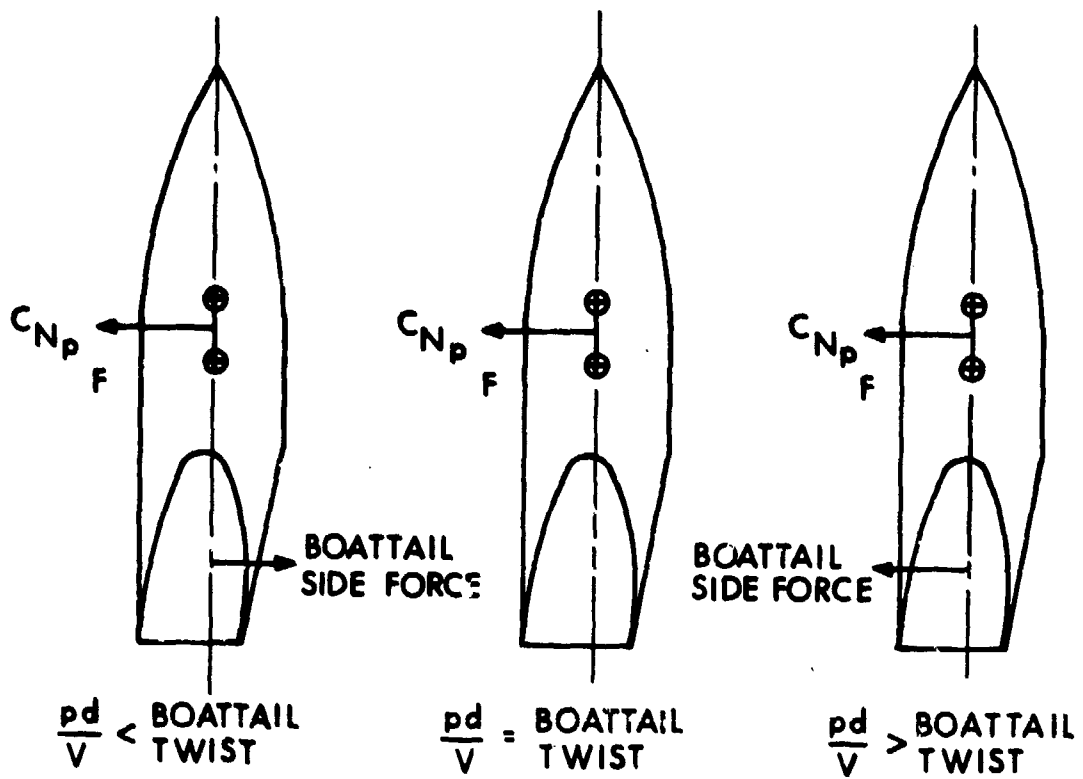


Figure 21. The Side and Magnus Forces on a Non-Conical Boattail Projectile, $\alpha > 0$



⊕
⊖
CENTER OF GRAVITY RANGE OF INTEREST

Figure 22. The Magnus and Side Forces Acting on a Triangular Boattailed Projectile at Various Spins (pd/V)

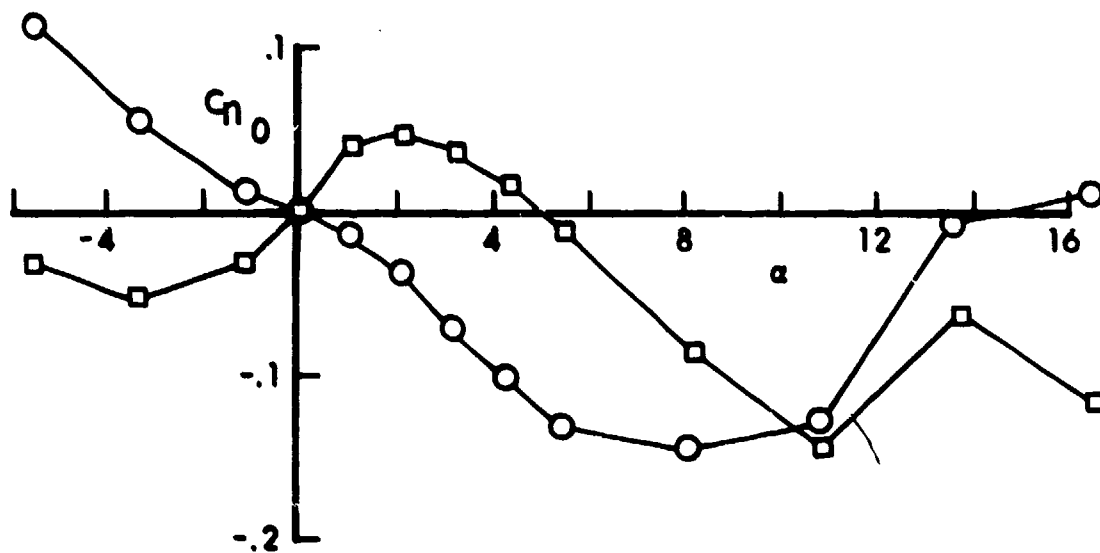
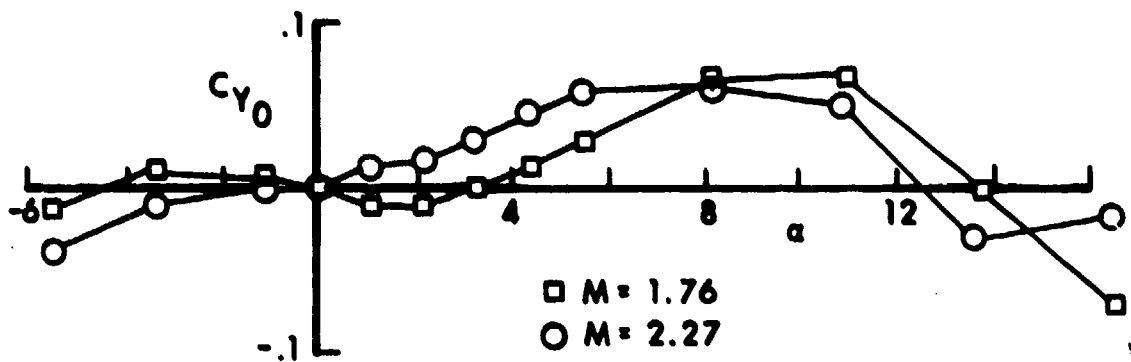


Figure 23. The Yawing Force and Moment Zero Spin Offset at $M = 1.75$ and 2.27 , $R_d = 1 \times 10^6$ of the NCB-A

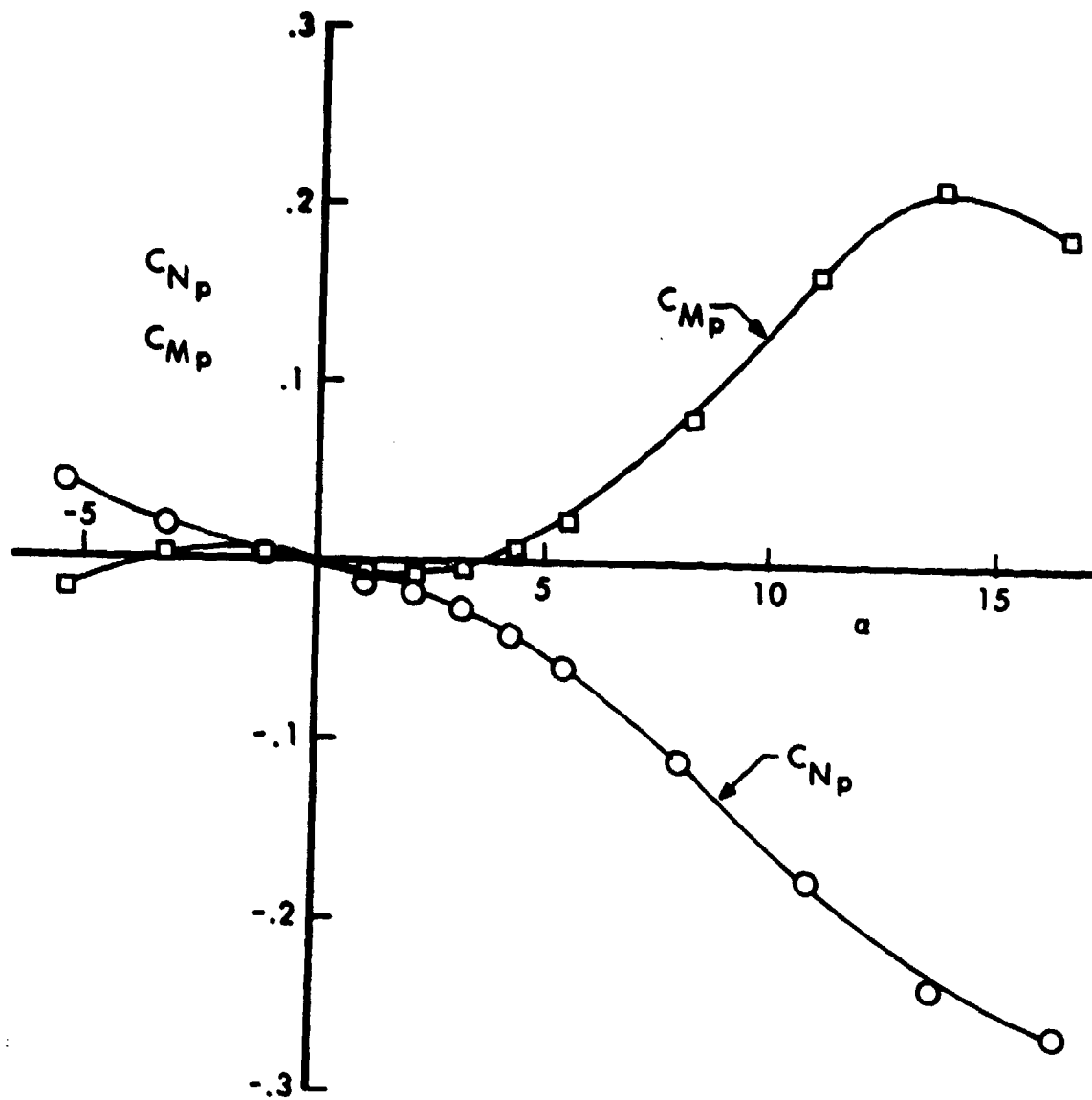


Figure 24. The Magnus Spin Slopes of the NCB-A at $M = 1.76$, $R_d = .97 \times 10^6$, $pd/V = .314$

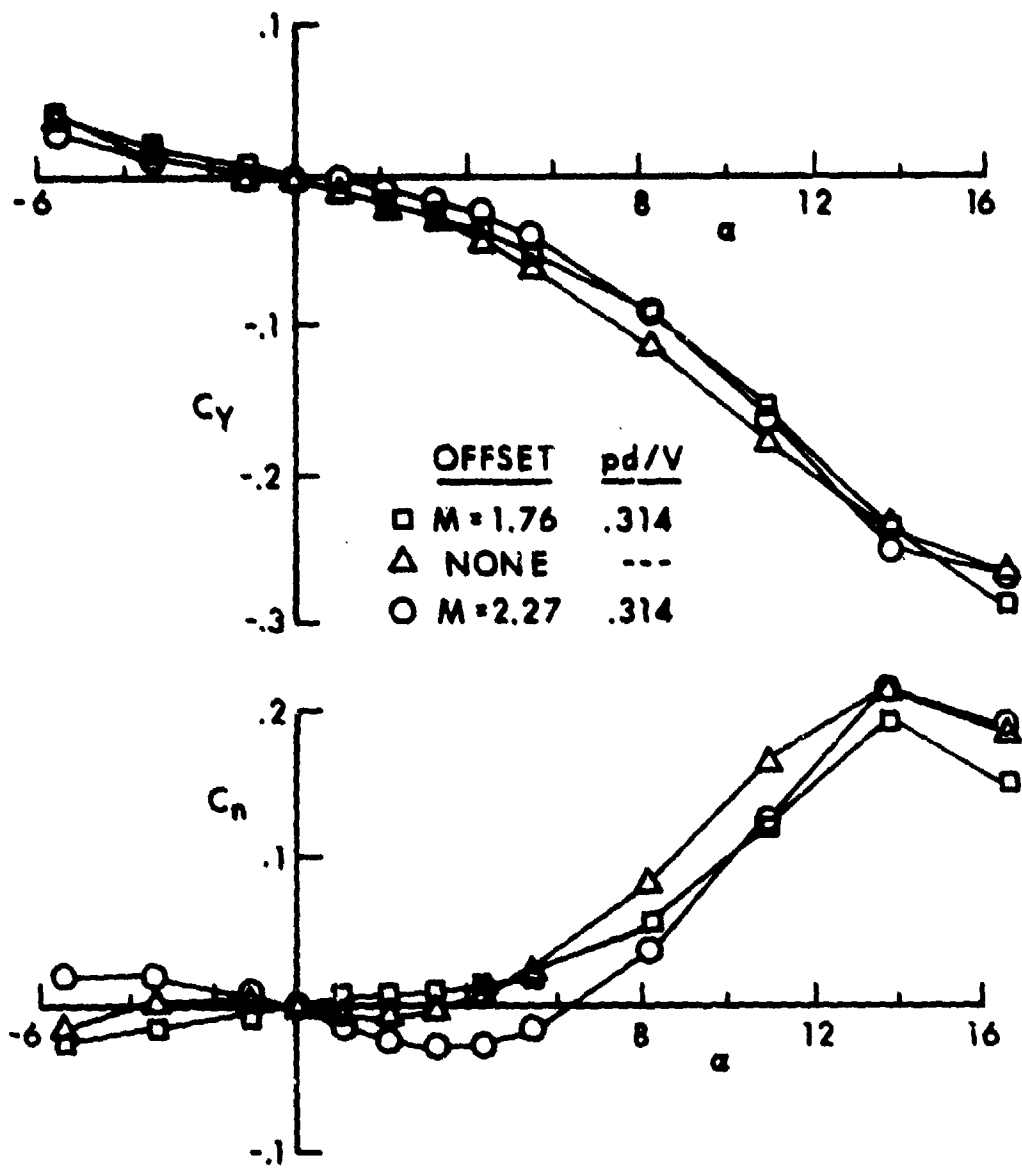


Figure 25. The Effect of Zero Spin Offset on the Yawing Force and Moment at $M = 1.76$ of the NCB-A

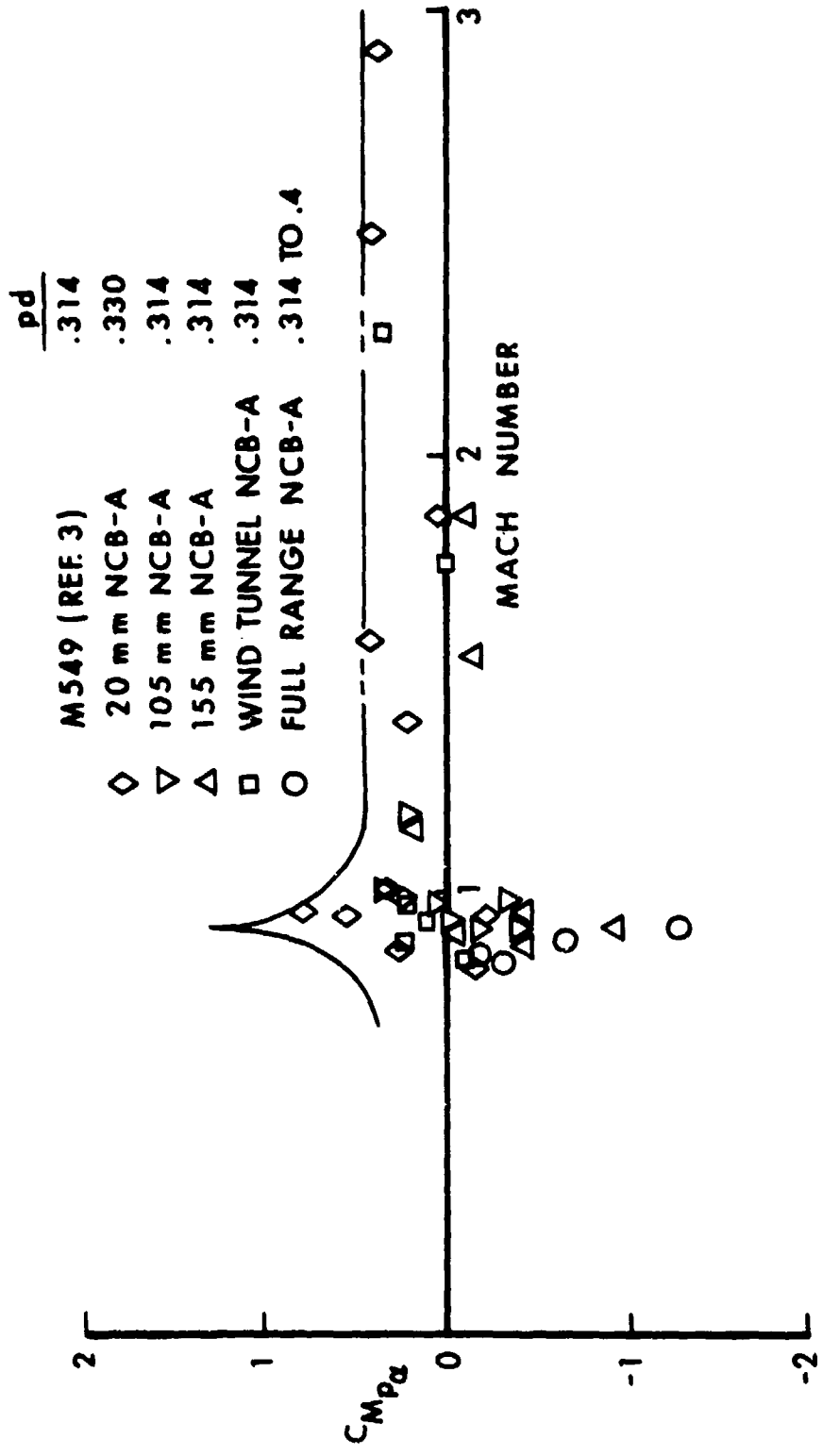


Figure 26. The Yawing Moment Coefficient of the NCB-A Compared to the M549 at Low Angles of Attack

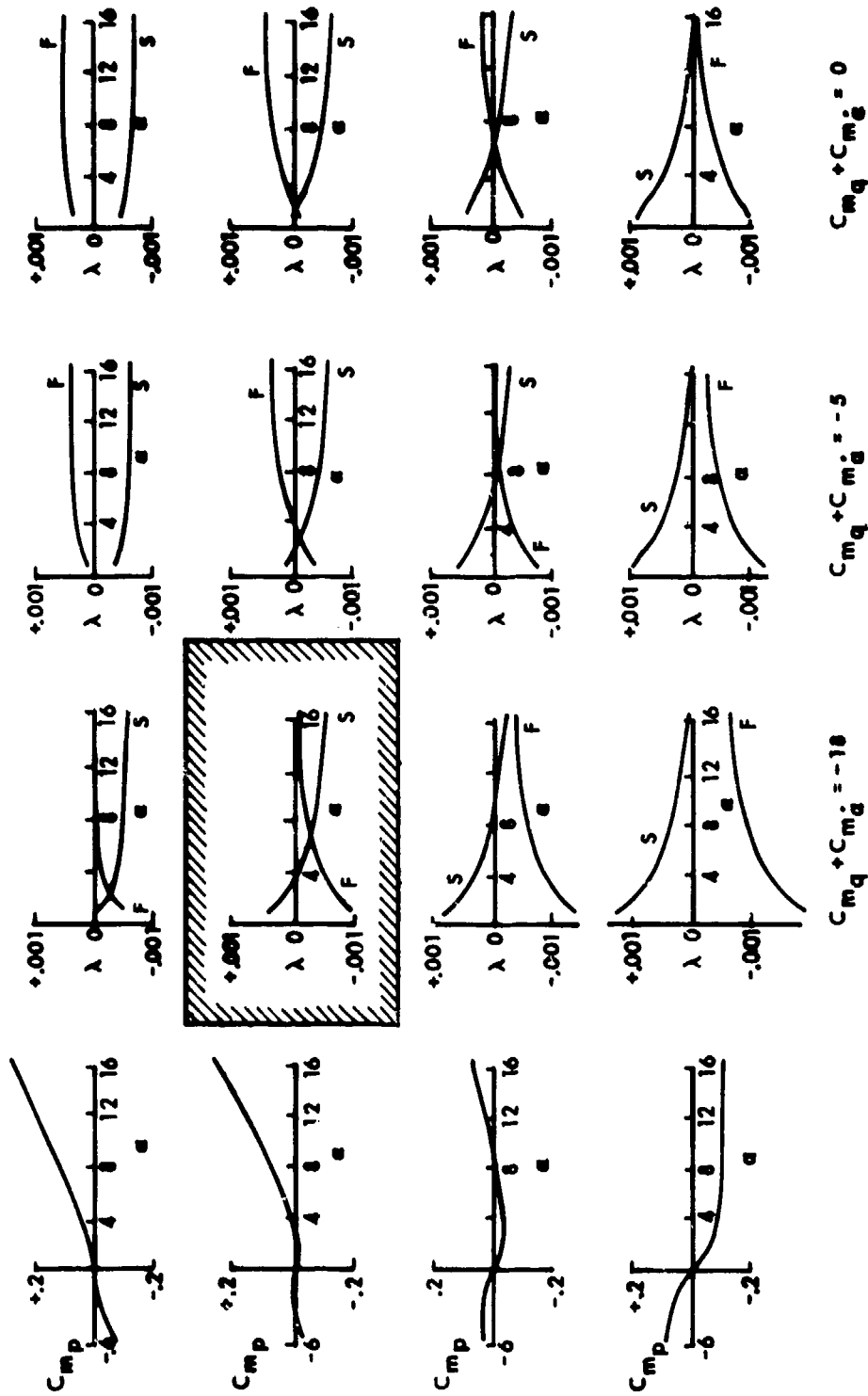


Figure 28. The Effect of the Side and Pitch Damping Moments on the Damping Rates (λ_F and λ_S) of the Epicyclic Arms, $H = 1.76$

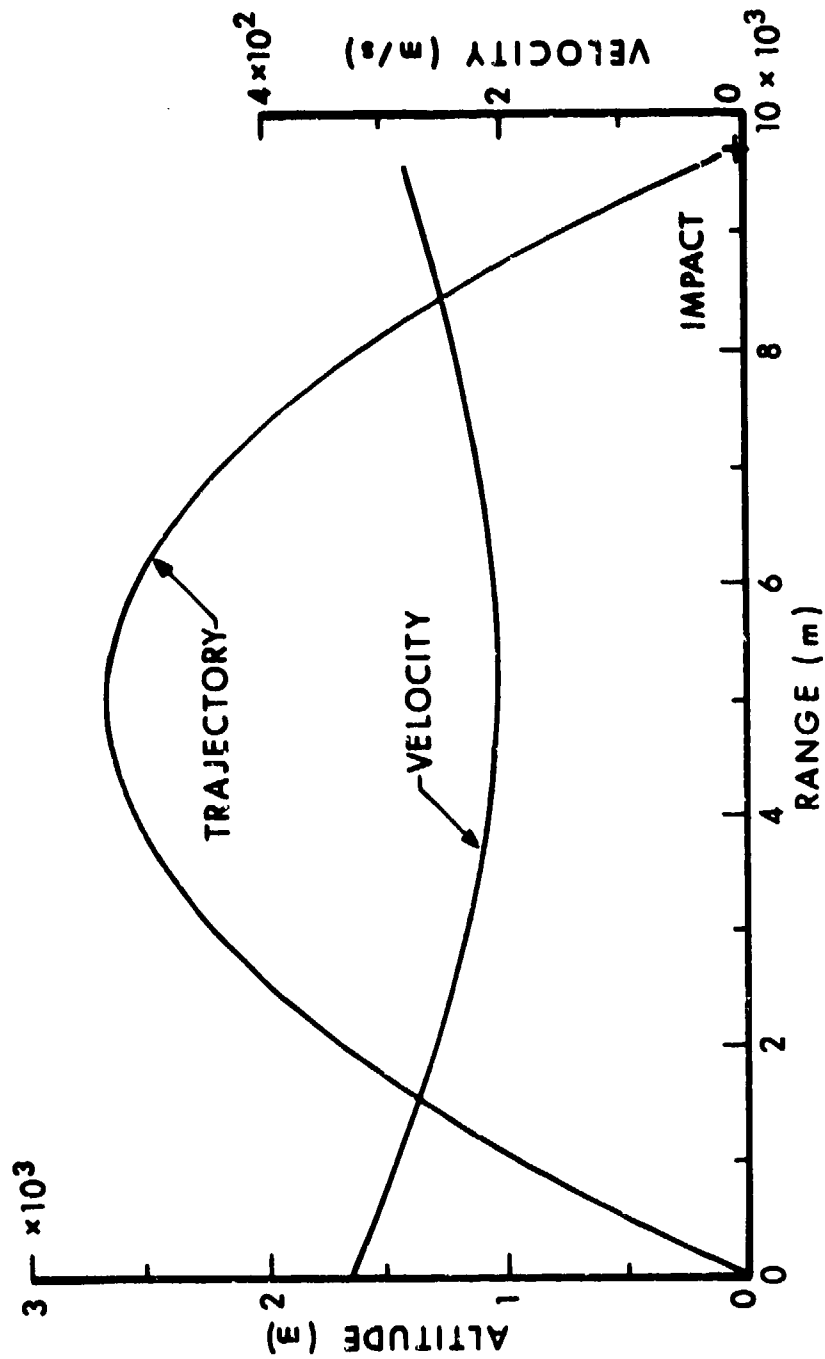


Figure 29a. Trajectory and Velocity of the NCB-A, $M = .98$,
 $Q.E. = 45^\circ$, $\rho = .997 \text{ kg/m}^3$ (Tonopah)

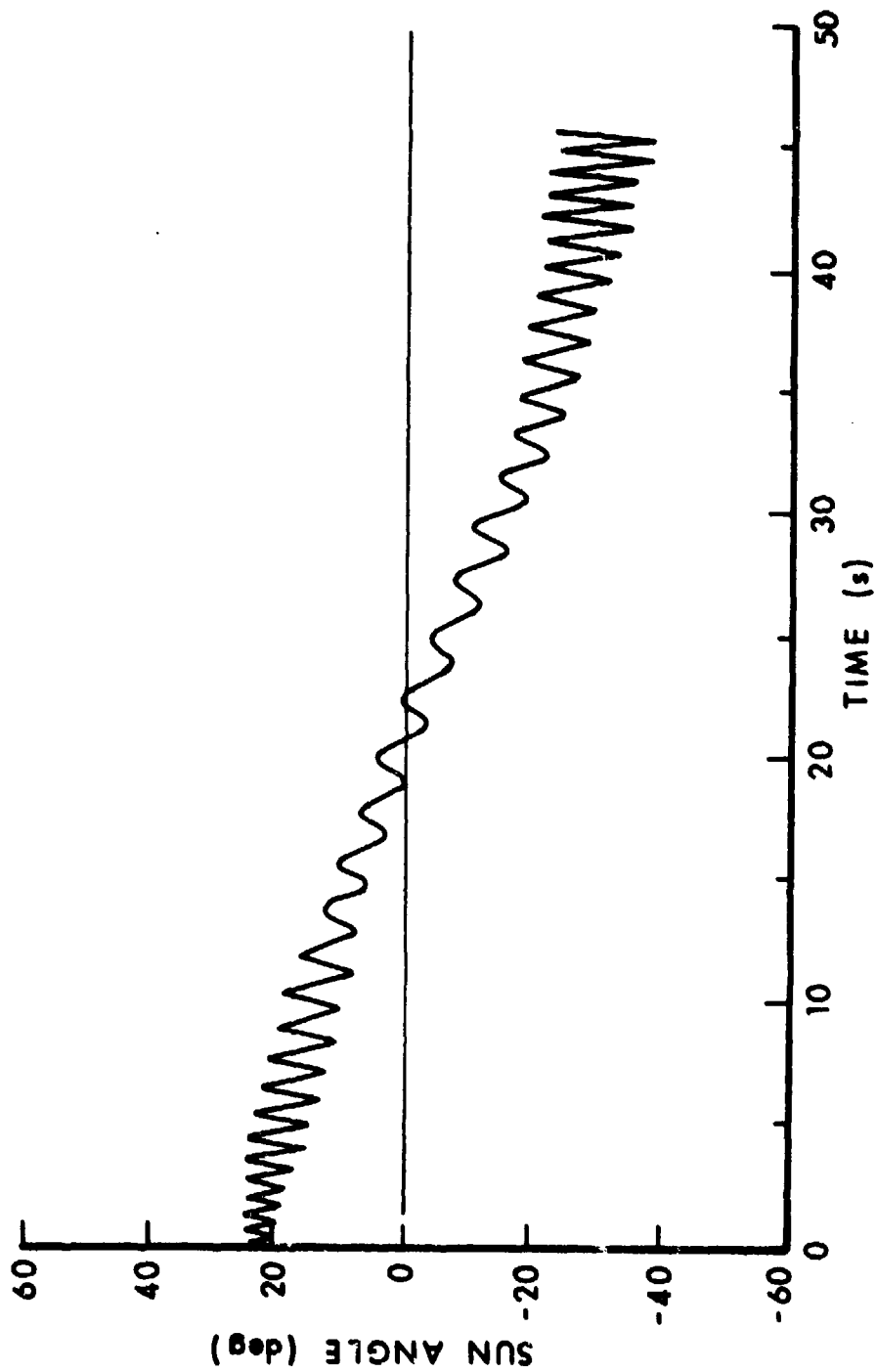


Figure 29b. The NCB-A Projectile Yawing Motion, Flight 11,
 $M = .98$, $Q.E. = 45^\circ$, $\rho = .997 \text{ kg/m}^3$ (Tonopah)

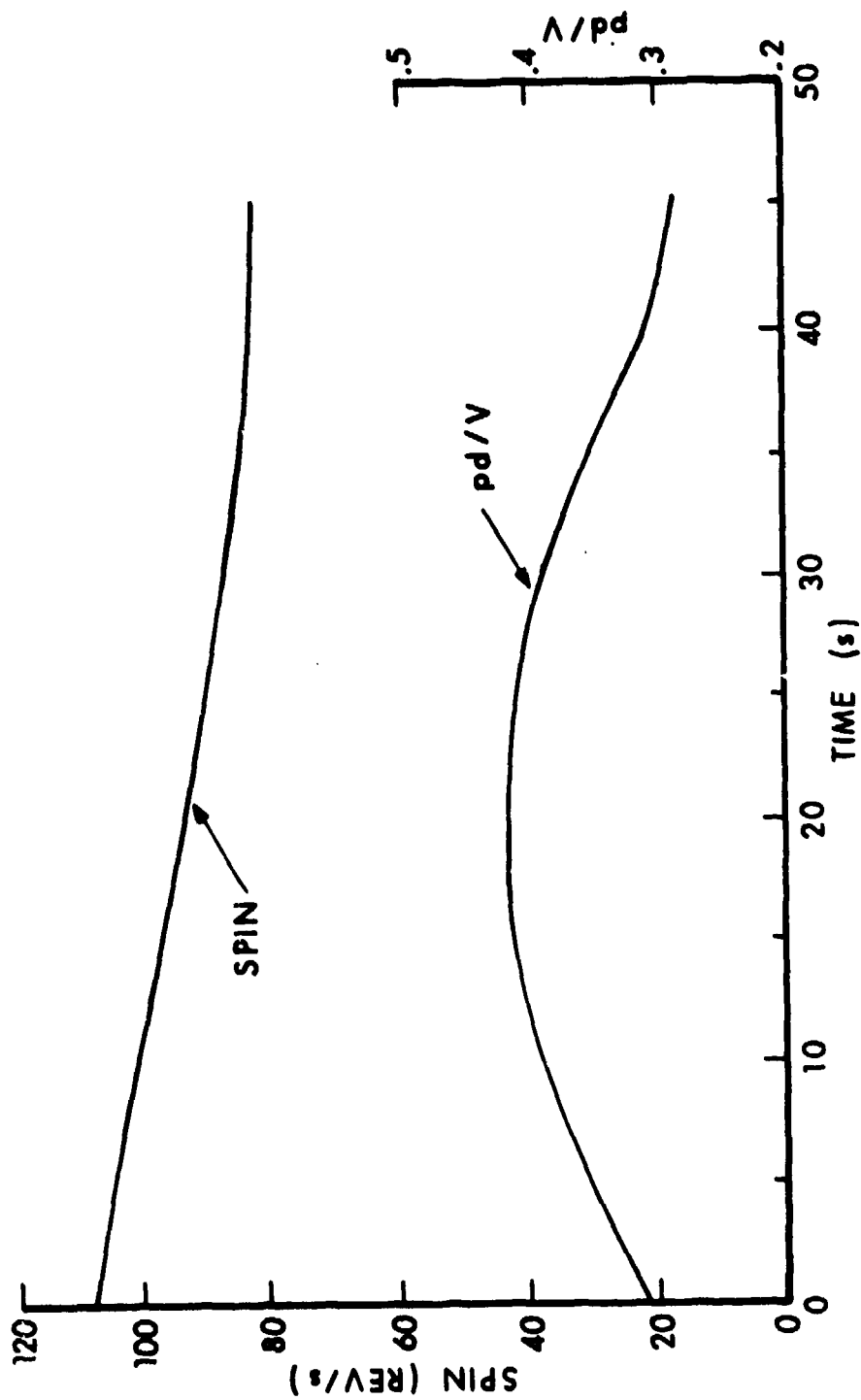


Figure 29c. The NCB-A Projectile Spin, Flight II, $M = .98$,
 Q.E. = 45° , $\rho = .997 \text{ kg/m}^3$ (Tonopah)

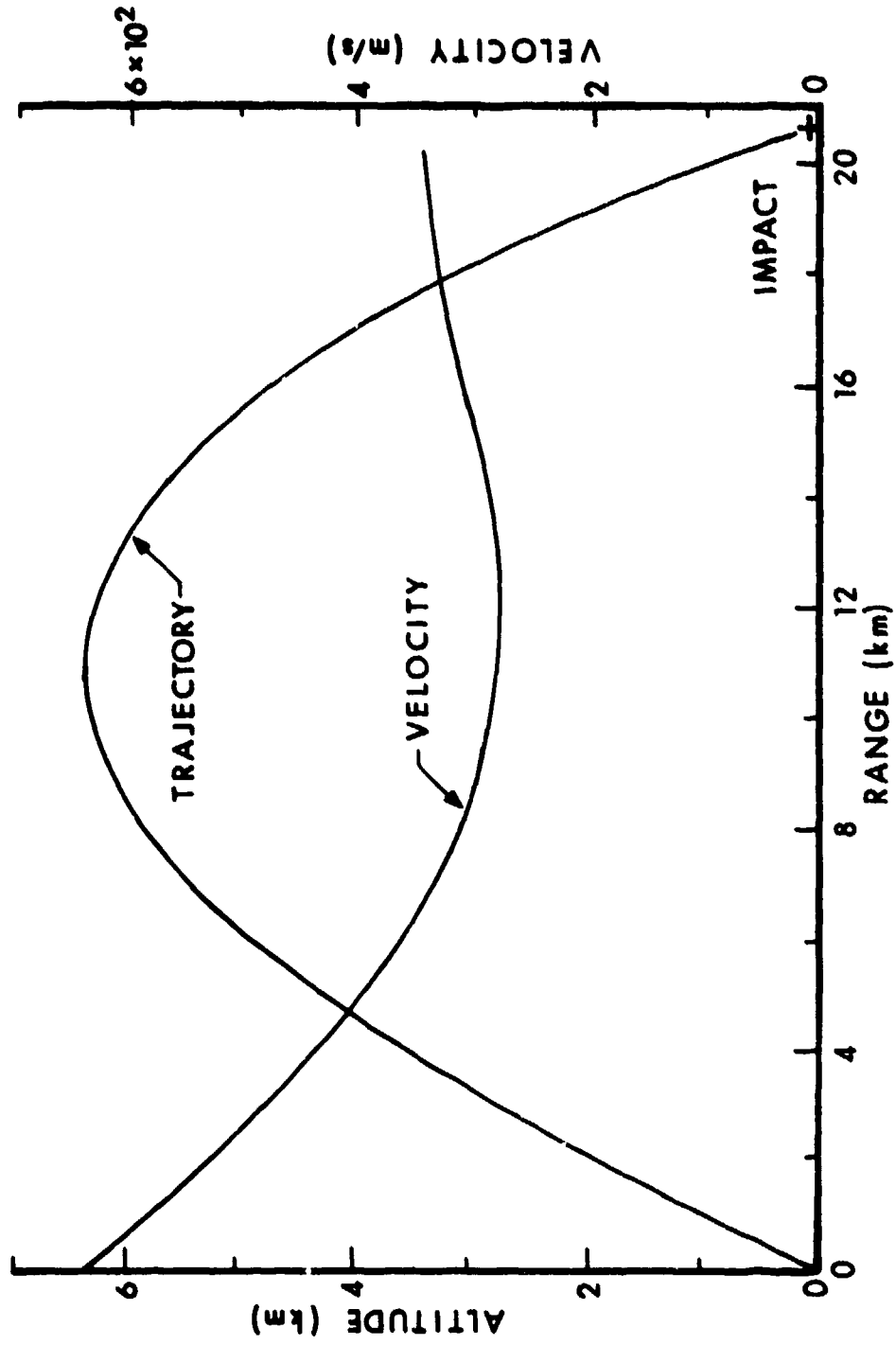


Figure 30a. Trajectory and Velocity of the NCB-A, $M = 1.8$,
 $Q.E. = 45^\circ$, $\rho = .997 \text{ kg/m}^3$ (Tonopah)

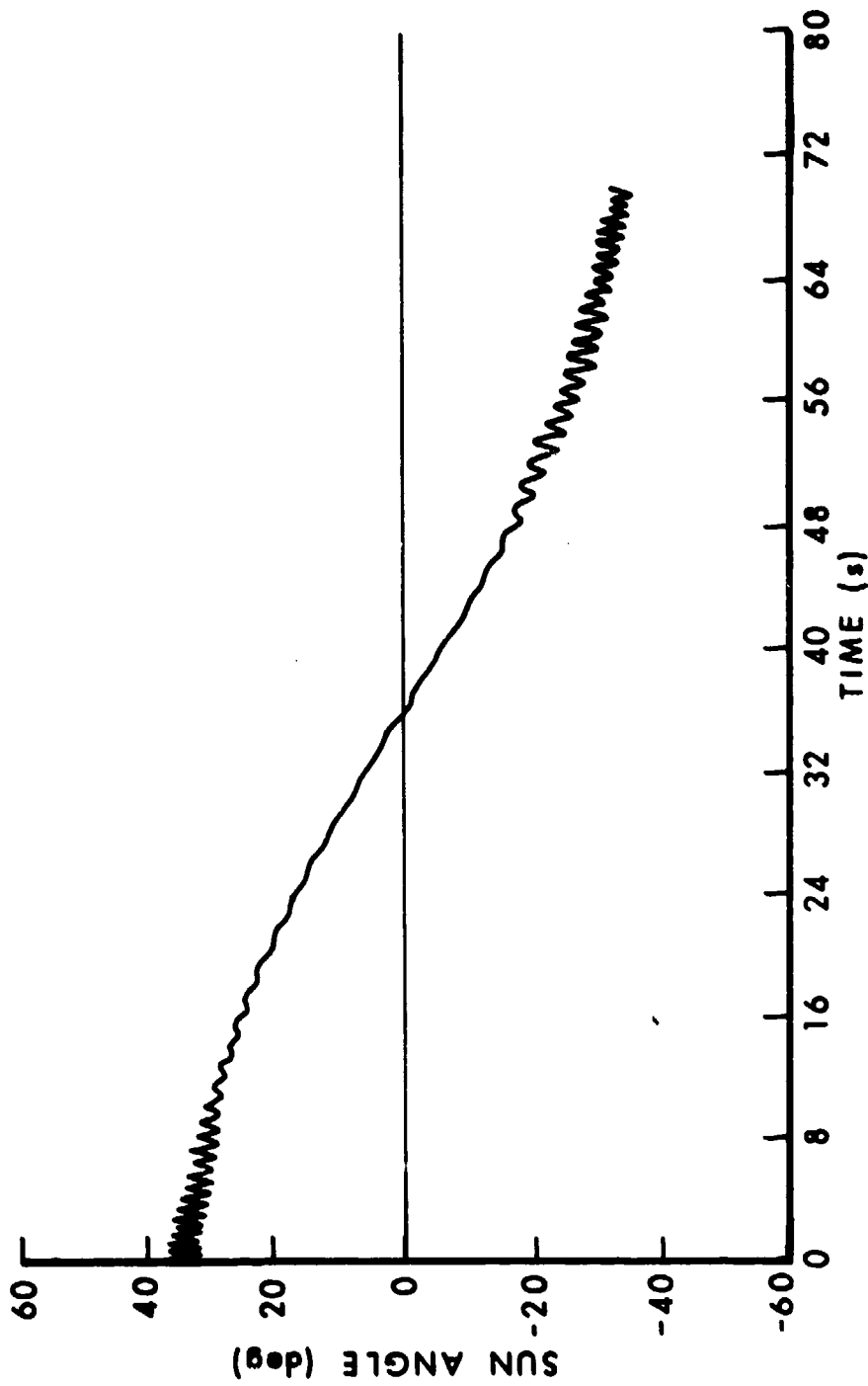


Figure 30b. The NCB-A Yawing Motion, Flight 20, $M = 1.8$,
 $Q.E. = 45^\circ$, $\rho = .997 \text{ kg/m}^3$ (Tonopah)

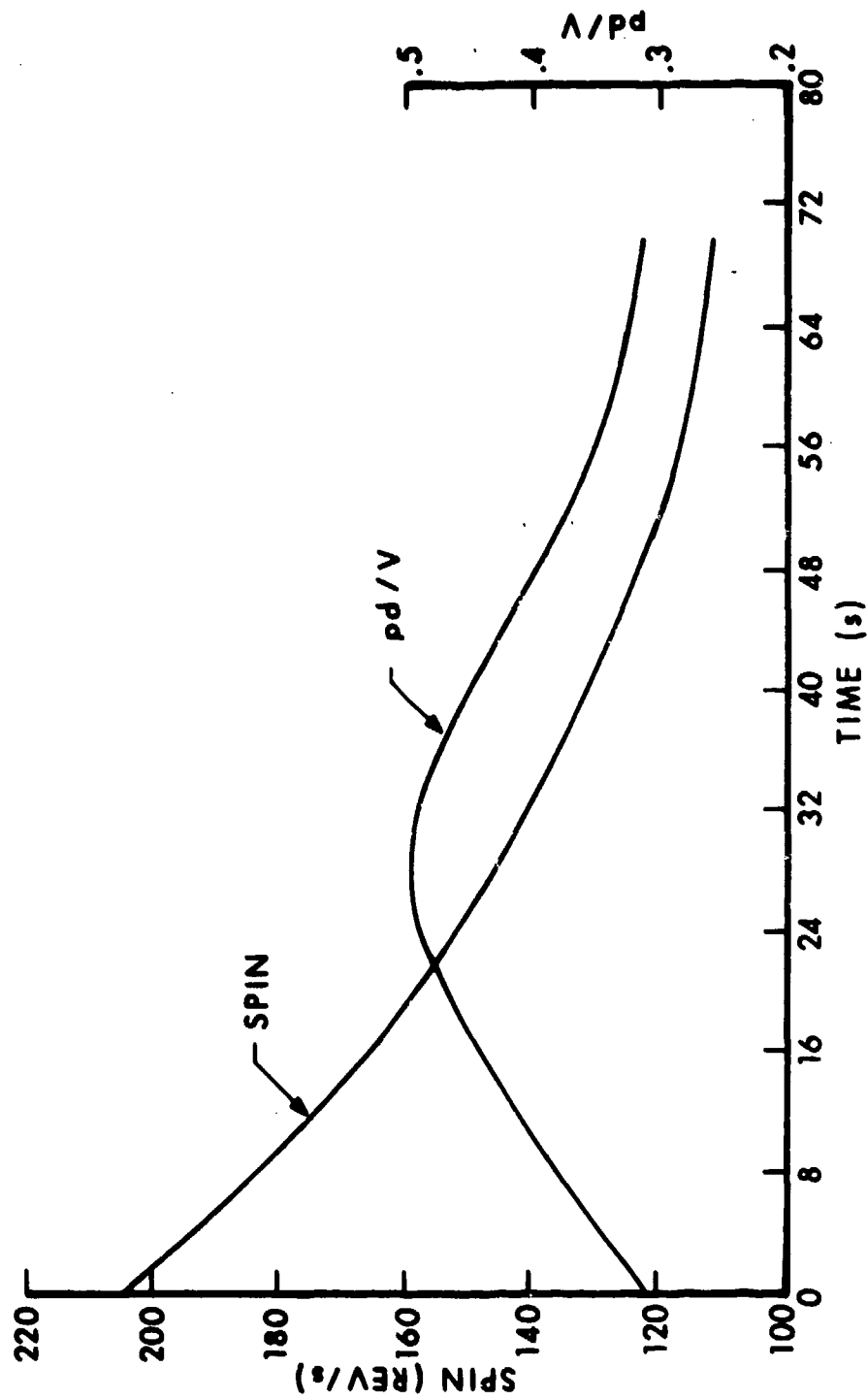
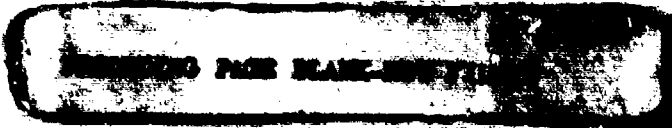


Figure 30c. The NCB-A Projectile Spin, Flight 20, $M = 1.8$,
 $Q.E. = 45^\circ$, $\rho = .997 \text{ kg/m}^3$ (Tonopah)

LIST OF SYMBOLS

C_D	<u>Drag</u> $\frac{1}{2} \rho V^2 S$	positive direction is aft
C_{D_0}		zero yaw drag coefficient
$C_{D_{\delta^2}}$		drag coefficient slope due to angle of attack (from $C_D = C_{D_0} + C_{D_{\delta^2}} \bar{\alpha}^2$)
C_M	<u>Pitching Moment</u> $\frac{1}{2} \rho V^2 S d$	positive moment is due to positive normal force ahead of the moment center
$\frac{dC_M}{d\alpha}$		near $\alpha = 0^\circ$ or $\frac{C_M}{\alpha}$ at large α (per radian)
C_{M_p}	<u>Magnus Moment</u> $\frac{1}{2} \rho V^2 S d \frac{pd}{V}$	positive moment is due to positive Magnus force ahead of the moment center
$\frac{dC_{M_p}}{d\alpha}$		near $\alpha = 0^\circ$ or $\frac{C_{M_p}}{\alpha}$ at large α (per radian)
$C_{M_q} + C_{M_{\dot{\alpha}}}$	<u>Damping Moment</u> $\frac{1}{2} \rho V^2 S d \frac{q_t d}{V}$	
C_N	<u>Normal Force</u> $\frac{1}{2} \rho V^2 S$	positive direction is up
$\frac{dC_N}{d\alpha}$		near $\alpha = 0^\circ$ or $\frac{C_N}{\alpha}$ at large α (per radian)
C_{N_p}	$\frac{C_Y \text{ at spin} - C_{Y_0}}{\frac{1}{2} \rho V^2 S \frac{pd}{V}}$	positive force is to right, looking upstream
$\frac{dC_{N_p}}{d\alpha}$		near $\alpha = 0^\circ$ or $\frac{C_{N_p}}{\alpha}$ at large α (per radian)



LIST OF SYMBOLS (Continued)

C_n	<u>Yawing Moment</u> $\frac{1}{2} \rho V^2 S d$
C_{n_0}	<u>Zero Spin Offset Yawing Moment</u> $\frac{1}{2} \rho V^2 S d \frac{pd}{V}$
C_{n_p}	C_n at Spin - C_{n_0} $\frac{1}{2} \rho V^2 S d \frac{pd}{V}$
C_{n_α}	linear term in $C_n = C_{n_\alpha} \alpha + C_{n_{\alpha^3}} \alpha^3$
$C_{n_{\alpha^3}}$	cubic term in $C_n = C_{n_\alpha} \alpha + C_{n_{\alpha^3}} \alpha^3$
C.P.N	normal force center of pressure
C_Y	<u>Yawing Force</u> $\frac{1}{2} \rho V^2 S$
C_{Y_0}	<u>Zero Spin Offset Yawing Force</u> $\frac{1}{2} \rho V^2 S$
d	body diameter and reference length
I_x	axial moment of inertia
I_y	transverse moment of inertia
K_x	axial radius of gyration = $\sqrt{I_x/m}$
K_y	transverse radius of gyration = $\sqrt{I_y/m}$
K_F	length of fast arm in epicyclic motion
K_S	length of slow arm in epicyclic motion
M	Mach number
m	mass of the projectile

LIST OF SYMBOLS (Concluded)

- p body axial spin rate, rad/sec (positive is clockwise looking upstream)
- p_0 projectile spin to match boattail twist at $V = V_0$
- q_t complex transverse angular velocity
- S body area = $\frac{\pi d^2}{4}$
- S_d dynamic stability =
$$\frac{2 (C_{L_\alpha} + k_x^{-2} C_{M_{p_\alpha}})}{C_{L_\alpha} - C_D - k_y^{-2} (C_{M_q} + C_{M_{\dot{\alpha}}})}$$
- S_g gyroscopic stability =
$$\frac{\frac{I_x}{I_y} \frac{pd^2}{V}}{4 \frac{\rho s d}{2m} \frac{d}{k_y} C_{M_\alpha}}$$
- V free stream velocity
- V_0 projectile velocity to match boattail twist at projectile spin p_0
- α angle of attack
- $\bar{\alpha}_t$ mean angle of attack during each flight
- δ cant angle of twisted surface $\tan^{-1} \frac{p_0 d}{2V_0}$
- ρ free stream air density
- λ_F damping rate of fast arm in epicyclic motion
- λ_S damping rate of slow arm in epicyclic motion

DISTRIBUTION LIST

<u>No. of Copies</u>	<u>Organization</u>	<u>No. of Copies</u>	<u>Organization</u>
12	Commander Defense Documentation Center ATTN: DDC-DDA Cameron Station Alexandria, VA 22314	4	Commander US Army Missile Research and Development Command ATTN: DRDMI-R DRDMI-YDL DRDMI-RDK Mr. R. Deep Mr. R. Becht Redstone Arsenal, AL 35809
1	Commander US Army Materiel Development and Readiness Command ATTN: DRCDMD-ST 5001 Eisenhower Avenue Alexandria, VA 22333	1	Commander US Army Tank Automotive Research & Development Command ATTN: DRDTA-UL Warren, MI 48090
1	Commander US Army Aviation Research and Development Command ATTN: DRSAV-E P.O. Box 209 St. Louis, MO 63166	8	Commander US Army Armament Research and Development Command ATTN: DRDAR-TSS (2 cys) DRDAR-LCA-F Mr. D. Mertz Mr. E. Falkowski Mr. A. Loeb Mr. R. Kline Mr. S. Kahn Mr. S. Wasserman Dover, NJ 07801
1	Director US Army Air Mobility Research and Development Laboratory Ames Research Center Moffett Field, CA 94035	1	Commander US Army Armament Materiel Readiness Command ATTN: DRSAR-LEP-L, Tech Lib Rock Island, IL 61299
1	Commander US Army Electronics Research and Development Command Technical Support Activity ATTN: DELSD-L Fort Monmouth, NJ 07703	1	Director US Army TRADOC Systems Analysis Activity ATTN: ATAA-SL, Tech Lib White Sands Missile Range NM 88002
1	Commander US Army Communications Research and Development Command ATTN: DRDCO-PPA-SA Fort Monmouth, NJ 07703		
1	Commander US Army Jefferson Proving Ground ATTN: STEJP-TD-D Madison, IN 47250		

DISTRIBUTION LIST

<u>No. of Copies</u>	<u>Organization</u>	<u>No. of Copies</u>	<u>Organization</u>
1	Commander US Army Natick Research and Development Command ATTN: DRXRE, Dr. D. Sieling Natick, MA 01762	1	Commander US Naval Weapons Center ATTN: Technical Library China Lake, CA 93555
1	Commander US Army Research Office P. O. Box 12211 Research Triangle Park NC 27709	1	AFATL (DLDL) Eglin AFB, FL 32542
3	Commander US Naval Air Systems Command ATTN: AIR-604 Washington, D. C. 20360	1	Director NASA Langley Research Center ATTN: MS-185, Tech Lib Langley Station Hampton, VA 23365
2	Commander David W. Taylor Naval Ship Research and Development Center ATTN: Dr. S. de los Santos Mr. Stanley Gottlieb Bethesda, Maryland 20084	1	Director NASA Ames Research Center ATTN: MS-202, Tech Lib Moffett Field, CA 94035
4	Commander US Naval Surface Weapons Center ATTN: Dr. T. Clare, Code DK20 Dr. P. Daniels Mr. D. A. Jones III Mr. L. Mason Dahlgren, VA 22448	1	Arnold Research Organization, Inc. von Karman Gas Dynamics Facility ATTN: Dr. John C. Adams, Jr. Aerodynamics Division Projects Branch Arnold AFS, TN 37389
4	Commander US Naval Surface Weapons Center ATTN: Code 312 Mr. S. Hastings Mr. F. Regan Mr. J. Knott Mr. R. Schlie Silver Spring, MD 20910	1	Calspan Corporation ATTN: Mr. J. Andes, Head Transonic Tunnel Dept. P. O. Box 235 Buffalo, NY 14221
		1	Honeywell, Inc. ATTN: Mr. George Stilley 600 Second Street, N. Hopkins, MN 55343
		1	Sandia Laboratories ATTN: Division No. 1331 Mr. H. R. Vaughn P. O. Box 5800 Albuquerque, NM 87115

DISTRIBUTION LIST

<u>No. of Copies</u>	<u>Organization</u>	<u>No. of Copies</u>	<u>Organization</u>
2	Space Research Corporation ATTN: Dr. G. V. Bull Dr. D. Lister North Jay Road P. O. Box 60 North Troy, VT 05859	1	University of Virginia Department of Aerospace Engineering and Engineering Physics ATTN: Prof. I. Jacobson Charlottesville, VA 22904
2	Massachusetts Institute of Technology ATTN: Prof. E. Covert Prof. C. Haldeman 77 Massachusetts Avenue Cambridge, MA 02139		<u>Aberdeen Proving Ground</u> Director, USAMSAA ATTN: Dr. J. Sperrazza DRXSJ-MP, H. Cohen
1	MIT/Lincoln Laboratories ATTN: Dr. Milan Vlainac Mail Stop D-382 P. O. Box 73 Lexington, MA 02173		Commander, USATECOM ATTN: DRSTE-TO-F
1	Rutgers University Mechanical, Industrial, and Aerospace Engineering Department ATTN: Dr. Robert H. Page New Brunswick, NJ 08903		Director, Weapons System Concepts Team Bldg. E3516, APG-EA ATTN: DRDAR-ACW Mr. M. Milier Mr. A. Flatau
1	University of Delaware Mechanical and Aerospace Engineering Department ATTN: Dr. J. E. Danberg Newark, DE 19711		Biophysics Lab. ATTN: Mr. W. Sacco Bldg. E3160